People's Democratic Republic of Algeria Ministry

of Higher Education and Scientific Research

University of Kasdi Merbah- Ouargla

Faculty of Hydrocarbons and Renewable Energy and Sciences

of the Earth and the Univers.

Departement of Renewable Energy.

Memory

Presented for obtaining a diploma

MASTER

Field: Mechanical Engineering.

Speciality: Renewable Energy in Mechanics.

Presented by:

Nihad BAHLOUL

Madjda BENNAI

Theme

Study of thermal efficiency of a double pass solar air collector

Publicly supported on: 05/06/2024

Before the jury composed of:

Dr. Abessamia Hadjadj	MCB	University Kasdi Merbah – Ouargla	Chairman
Dr. Amar Rouag	MCA	University Kasdi Merbah – Ouargla	Supervisor
Dr. Mohamed Dernouni	MCB	University Kasdi Merbah – Ouargla	Examiner

Academic year: 2023/2024

إهداء

بسم الله وصلاة والسلام على رسول الله

احمد الله عز وجل على منه وعونه لإتمام هذا العمل

اهدي هذا العمل الى الوالدين العزيزين الذين اعانوني و شجعوني على الاستمرار

الى اخوتي و العائلتي الكريمة حفظهم الله .

نهاد بهلول

الاهداء

من قال أنا لها "نالها".

لم تكن الرحلة قصيرة ولا ينبغي لها أن تكون.

لم يكن الحلم قريبًا ولا الطريق محفوفًا بالتسهيلات، لكني فعلتها ونلتها.

الحمد لله حبًا وشكرًا وامتنانًا، الذي بفضله ها أنا اليوم أنظر إلى حلم طال انتظاره وقد أصبح واقعًا أفتخر به

إلى ملاكي الطاهر، وقوتي بعد الله، داعمتي الأولى والأبدية "أمي"، أهديك هذا الإنجاز الذي لولا تضحياتك لما كان له وجود. ممتنة لأن الله اصطفاك لي من بين البشر أماً يا خير سند وعوض

."إلى من دعمني بلا حدود وأعطاني بلا مقابل " أبي "

وإلى من آمنوا بقدراتي، زهراتي " أخواتي "

ولكل من أعطاني يد العون من قريب أو بعيد وساعدني في إنجاز هذه المذكرة

ماجدة بناي

Acknowledgments

Praise be to God who gave us the courage and determination to complete this humble work.

we would like to extend special thanks to Dr Amar Rouag, who was the main supervisor of our thesis. We deeply grateful to him for his valuable advice and guidance which contributed greatly to achieving excellent results.

We thank our colleagues who helped us in this work, and we would also like to express our gratitude to the Renewable Energy Department management team for their assistance.

Finally, we thank everyone who contributed directly or indirectly to the completion of this work.

Summary

List of Table

List of Figures

List of abbreviations

Nomenclature Symbols	Definition	Unit
T_1	Glass tempertaure	(K)
T_2	Absorber plate temperature	(K)
T_3	Bottom temperature	(K)
T_f	Air flow temperature	(K)
T_a	Ambient temperature	(K)
T_s	Temperature of sky	((K)
I	Incident solar radiation	(W/m^2)
h_1	Convective heat transfer coefficient between glass cover and air flow	(W/m^2K)
h_2	Convective heat transfer coefficient between absorber plate and First air flow	(W/m^2K)
h_3	Convective heat transfer coefficient between absorber plate and Second air flow	(W/m^2K)
h_4	Convective heat transfer coefficient between Second air flow and bottom plate	(W/m^2K)
hr_{21}	Radiation heat transfer coefficients between glass cover and absorber plate	(W/m^2K)
hr_{23}	*radiative heat transfer between the absorber and the lower plate.*	(W/m^2K)
hr_s	Radiation heat transfer coefficients between glass cover and sky	(W/m^2K)
hw	Heat transfer coefficient of wind	((W/m^2K)
Cp	Heat capacity of air	(J/Kg K)
Kf	Thermal conductivity of air flow	(W/m K)
kbi	Thermal conductivity of insulation	(W/m K)
Ub	Bottom heat loss coefficient	(W/m^2K)
UL	Top heat loss coefficient	(W/m^2K)
$\dot{m}$	Air mass flow rate	(Kg/s)
V	Wind velocity	(m/s)
Re	Reynolds number	
Nu	Nusselt number	

L	Length of collector	(m)
W	Width collector	(m)
Xbi	Insulation thickness	(m)
d	Spacing between absorber and glass	(m)
Dh	Hydrolic diameter	(m)
A	Cross section of flow area	(m^2)
P	‘Wetted perimeter	(m)
Q	Heat transferred to the air and can be used.”	
ε1	Glass cover emissivity	
ε2	Absorber plate emissivity	
α1	Abrober plate emissivity	
τ	Transmissivity	
ρ	Density of air stream	(Kg/m^3)
σ	Constant of Stefan-Boltzmann	
μ	A stream of air's dynamic viscosity	($Kg/m\ s^2$).
Indices	Definition	
f, fi, fs	Fluid, initial fluid, outlet fluid	
SAH	solar air heating	
DPSAH	Double pass solar air heating	
SPSAH	Singel pass solar air heating	
EBEs	Energy balanc equations	

General Introduction

General Introduction

In the midst of the global energy crisis that has worsened over the past two decades, the search for sustainable alternatives to traditional energy sources has become imperative. Solar energy stands out as a promising solution, as it provides a clean, inexhaustible energy source that can be used in a variety of thermal and electrical applications.

Solar technology is advancing rapidly, resulting in lower installation and operating costs, as well as increased efficiency. The use of solar energy converted into heat in the industrial sector is considered one of the most promising applications, as it provides great opportunities to enhance energy efficiency and reduce harmful emissions. This includes heating, drying and cooling, which contributes to reducing dependence on fossil fuels and achieving sustainable development goals.

Heat transfer is of utmost importance in thermal systems in general and insulated systems in particular. It requires a comprehensive understanding of different thermal properties and accuracy in their evaluation in sensitive systems. This explains the huge amount of previous and current research on the same topic.

In the context of the global emphasis on switching to environmentally friendly energy sources, solar thermal energy systems can be employed with SAH for some functions such as building heating, food drying, desalination, and air conditioning [1]. Solar air collectors were utilized as the primary component in a variety of solar drying systems for agricultural commodities [2]. Traditional solar air heaters have inherent drawbacks in terms of reduced thermal efficiency. A variety of solar air collector configurations have been created in an effort to find the best design for various purposes. Numerous solar collector designs havebeen suggested, among which are multi-pass solar collectors.

In previous research, researchers used several simplified hypotheses to accurately analyze the behavior of the complex, and it is necessary to study the factors affecting the efficiency of thesolar collector.

Our goal is to study the thermal performance of DPSAH and the influence of internal and external factors on their efficiency in stationary conditions. Specifically, we aim to estimate the heat transfer coefficients by measuring the temperature of the various components of DPSAH. In addition, the goal is to reach the maximum amount of solar energy at the lowest costs.

This dissertation is structured into four chapters:

The first chapter addresses the study of solar potentials, presenting some common astronomical concepts and definitions used in the solar field. In this chapter, we will also review various solar applications and provide an overview of the technologies that enable the conversion of solar energy into thermal energy using different types of SAH.

The second chapter provides a literature review of the various studies conducted on DPSAH

The third chapter focuses on presenting the thermal balance equations for DPSAH in a steady state, accompanied by a numerical simulation of the thermal phenomenon.

In the final chapter, we present the results and discussions derived from the numerical simulation using Matlab.

Chapter I: Generalities on solar collectors

I.1 Introduction

Fossil fuels have been used as the main source of energy for a long time, highlighting challenges such as depletion of reserves, environmental impacts, price volatility. In this context, our dependence on renewable and sustainable energy sources, such as solar thermal energy, has increased due to their efficiency and availability. Solar thermal energy has been developed as an effective alternative, as our attention is focused on its systems and its role in using and harnessing solar heat in various applications such as water heating, drying, and heating.

Solar air collectors (SAC) are an innovative technology in the field of solar thermal energy, as they are used to harness air and convert it into usable heat. This technology represents an effective and environmentally friendly solution to meet thermal needs

In this chapter, we will deal with the field of solar energy and solar air collectors, their principle of operation, types and applications [3].

I.2 Solar field

Solar field a set of data that describes the evolution of available solar radiation over a specific period. It is used to simulate the operation of a solar energy system and to obtain the highest possible accuracy while taking into account the required demand to be met.

After an evaluation via satellites, the German Aerospace Center (DLR) concluded that Algeria is a country rich in solar energy potential. It has the largest solar energy potential in the Mediterranean basin and is located in a privileged geographical area with high solar radiation, 169.000 TWh/an for solar thermal energy and 13,9 TWh/an for solar photovoltaic energy. Algeria's solar energy potential is equivale0nt to 10 large natural gas fields, making it a huge source of clean energy.

Table I. 1: the different levels of sunshine in the Algerian regions [4].

Regions	**Coastal region**	**Highlands**	**Sahara**
Area (%)	4	10	86
Average duration of sunshine (h/year)	2650	3000	3500
Average energy received (Kwh/m^2/an)	1700	1900	2650

The Algerian desert is characterized by the highest duration of insolation in the world,

which reaches a value 3500h/an and range from 8h/day to 12 h/day during the summer and the duration of insolation in the Far South decreases to 6 h/day, as the region of Adrar is considered the sunniest in Algeria [4].

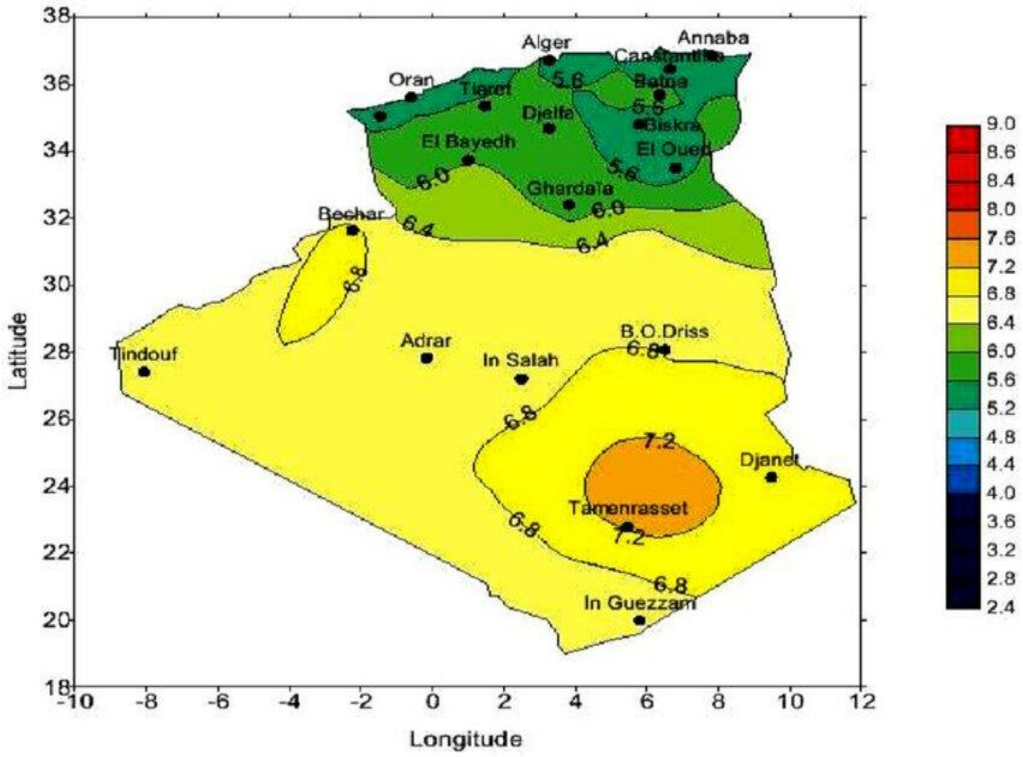

Figure I. 1: Global solar irradiation received by Algeria: annual average [4].

I.2.1 Solar energy

The sun is considered a primary source of free and renewable energy, delivering vast amounts of solar energy to the Earth daily in the form of absorbable radiation. Advanced techniques are employed to efficiently and sustainably generate electricity and heat from solar energy, with the effectiveness of these technologies proven and widely used worldwide as sustainable alternatives for energy.

I.2.1.1 Special properties

The only external energy source on Earth is solar energy, it represents The following characteristics:

Approximately four million exajoules 1×0^{18} EJ of solar energy reach the Earth annually, roughly 5×10^4 EJ of which is received in the Earth's atmosphere per year. This contributes to radiation reaching the Earth's surface at an average rate of about 342 W/m^2, with the amount of solar radiation received varying by region. The temperature of the sun's black body is approximately 5800 K. It takes about 8 minutes for the radiation, emitted in the form of

electromagnetic waves, to reach the Earth, traveling at a speed of 300,000 Km/s, Notably, 98% of the energy emitted by the sun falls within the wavelength range of 0.25 to 3 μm. Solar energy presents a viable option to meet the increasing demand for future energy, given its availability and positive impact on public health and the environment, including animals, plants, and minimal greenhouse gas emissions. Therefore, solar energy represents a promising, economical, and socially beneficial solution toward sustainable development and addressing current challenges of global warming [5, 6].

I.2.1.2 The caption

There are many technologies for capturing solar energy, including:

- **Solar thermal energy**

Solar thermal energy is defined as the process of converting solar energy into energy

Thermocouples, which are used in several diverse areas, including:

- Direct uses of heat: solar water heaters, solar heating systems, fireplace and solar drying.
- Indirect use of heat: solar power plants Thermodynamics, solar cooling systems.

- **Thermodynamic solar energy**

This technology is based on the conversion of solar thermal energy into electricity, using the same principle of operation as conventional power plants, with the replacement of fossil fuel, using Solar thermal power production plants.

Three main types of thermodynamic solar power plants are used:

- Central parabolic cylindrical sensors: temperatures in them reach between 300 and 350 °C.

- Equivalent collection stations: where temperatures of 1000 °C are reached or More.

- Tower power plants: the temperature produced in them reaches 1000 °C.

- **Solar photovoltaic energy.**

This technology produces electricity by converting part of the solar radiation into electrical energy by a photovoltaic cell. The latter are based on the photoelectric effect, and consist of a layer of a semiconductor material, such as silicon or gallium arsenide [7].

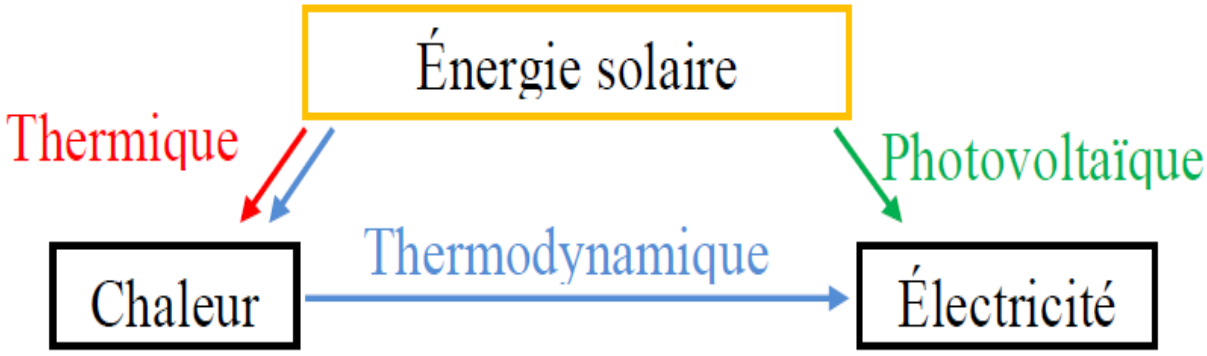

Figure I. 2: Solar energy conversion sector [7].

I.2.2 Earth's motion

The Earth revolves around the sun in a journey that takes one year, with its tilt angle reaching 23.5 °. It also rotates around its axis every 365.25 days, at a speed of approximately 30 Km/s. The Earth's path around the sun is an elliptical orbit with the sun at one of the foci, and the average distance between the Earth and the sun ranges between 144 and 154 MKm.

The Earth is closest to the sun on December 21, the winter solstice, while it is farthest from it on June 21, the summer solstice. This is expressed by the solar declination (δ), which varies throughout the year, ranging from -23° 27' at the winter solstice to +23° 27' at the summer solstice, and zero at the equinoxes.

A pyranometer is used to measure the solar radiation falling on the Earth's surface, converting the radiation into heat through a horizontal blackened surface, and this rise in temperature is measured using a thermal column consisting of several connected thermal couples in series [6].

Geographical coordinates are determined using latitude, longitude, and altitude (h or Z), where longitude is the angle between the location's longitude and the meridian, and latitude is the angle between the location and the equator.

The solar altitude (in degrees) is the angle between horizontal levels and the direction of the sun, ranging from 90° (zenith) at sunrise and sunset to -90 ° (nadir) at its lowest point in the sky [8].

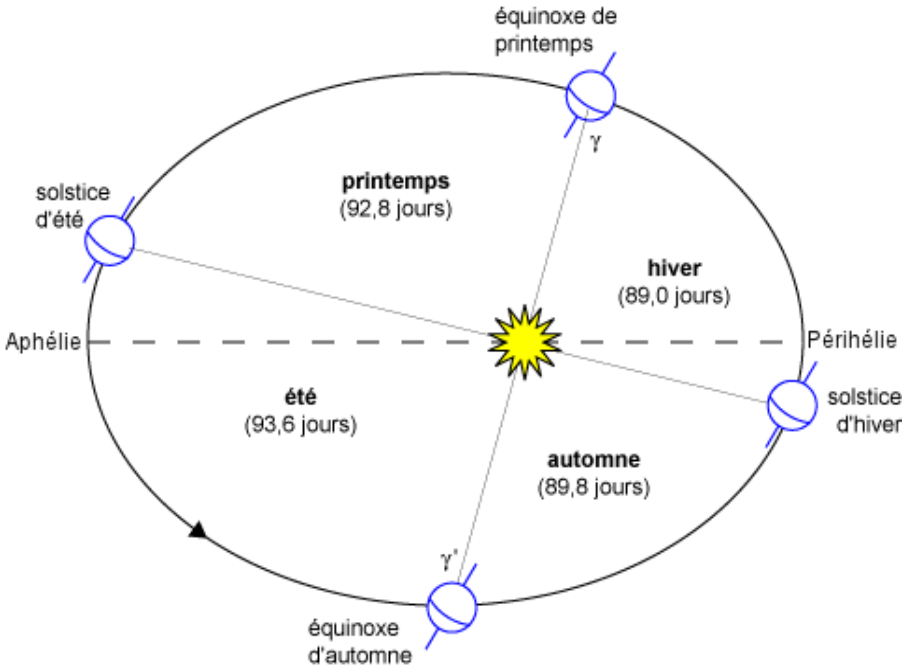

Figure I. 3: Motion of the earth around the sun [6].

I.3 Air solar collectors

Solar air collectors are an essential part of the technologies used to harvest solar energy and convert it into heat. they rely on airflow as a working medium. The resulting heat is used for drying industrial products and heating buildings [9].

Different components of a flat plate solar collector system consist of four parts:

- **Glass Cover**

The glass cover receives direct solar radiation and plays a role in ensuring the efficient transfer of radiation to the absorber. The glass cover can be single, double, or triple to enhance energy absorption efficiency and reduce losses to the outside.

- **The heat transfer fluid**

Water and air are commonly used as heat transfer fluids circulated by the collector to the outside. They are preferred due to their low cost and large storage and heat exchange capacity.

- **Absorber**

The absorber is made of materials with high solar energy absorption capabilities, such as black metal sheets. It is a crucial element in the collector as it efficiently collects as much heat as possible and transfers it to various collector components through heat transfer mechanisms (fluid convection, radiation, or conduction). The absorber should have maximum heat exchange with the heat transfer fluid to increase collector efficiency, improve heat exchange with the fluid, and minimize losses to the outside.

- **Insulation**

It is used for the purpose of storing the thermal energy captured from sunlight. In order to maximize this energy, it is essential to use sufficient insulation materials to minimize losses to the ouchannels [10].

- **air blowers in active systems.**

Several factors affect the performance and efficiency of the air collector, such as its collector length, collector depth, type of absorber plate, glass cover plate, wind speed etc.

The solar air heater is considered to have low thermal efficiency, primarily due to poor heat transfer between the absorber plate and the air flowing in the channel. In order to improve system and make it more efficient for solar energy utilization, enhance thermal performance, and increase effectiveness, it is necessary to enhance the heat transfer rate from the absorber plate to the airflow in the solar air heater channel. This can be achieved by improving heat transfer by conduction through enhancing the heat absorber, as it is the main component of the solar air collector, or by increasing the heat transfer area [11].

I.3.1 Principle of operation of air solar collectors

Air-based solar collectors are used in various applications that require low and medium temperatures. Their function is to convert the solar energy falling on them into thermal energy, and they rely on the ability of the collector surface to absorb sunlight.

The absorber of the air solar collector absorbs the sun's energy and raises the temperature of the air passing through it, and re-emits the other part as infrared radiation. Therefore, the optimal absorbing surface is one that absorbs the visible spectrum to a greater extent and emits infrared radiation weakly.

A hollow polycarbonate cover is placed above the absorbing surface, which is transparent to visible sunlight and opaque to infrared radiation, which it absorbs and returns to the absorbing surface. This allows the radiation to be trapped between the absorbing surface and the cover, which increases the temperature of the absorbing surface. Lateral and rear insulation is provided by walls covered with thermal insulation materials. Heat exchange can take place between the sensor components by convection, conduction, and radiation.

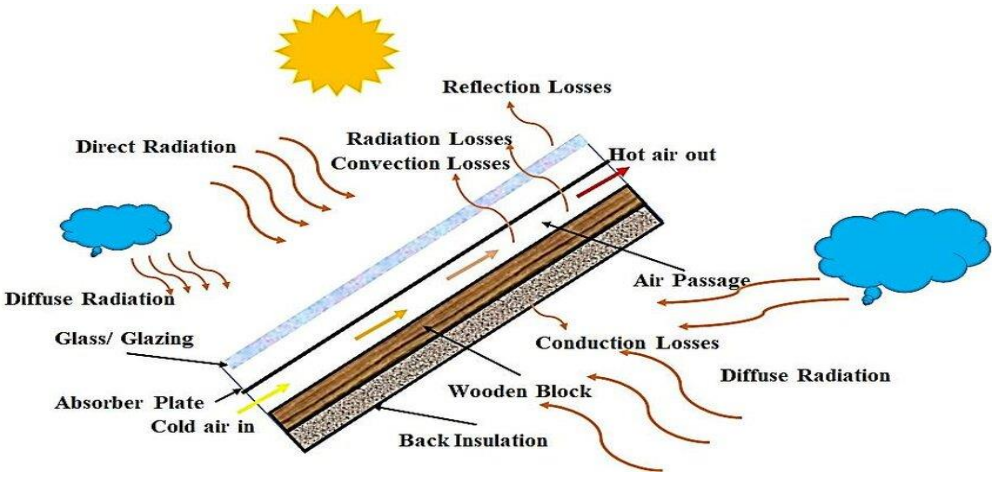

Figure I. 4: Principle of operation of air solar collectors [12].

I.3.2 Advantages and disadvantages

Advantages

- Air is used as a heat transfer fluid in the system due to its efficiency in reducing manufacturing and maintenance costs. Additionally, air does not pose any issues with freezing or boiling, eliminating the need for antifreeze or safety systems against overpressure.
- Its applications are versatile, as hot air can be used for various purposes such as home heating or industrial applications.
- Reduction in manufacturing and maintenance costs.
- Lightweight air sensor and easy installation.
- Environmentally friendly and sustainable.

disadvantages

- Solar energy conversion efficiency into air heat is lower compared to some other technologies.
- Requires high volume flow rates, hence increased electricity consumption (fan).
- Effects of different weather conditions [13].

I.3.3 Applications of air solar collectors

Solar air collectors have been used in a variety of the most widespread applications, such as heating, air conditioning and drying، Production of mechanical energy, etc.

I.3.3.1 Heating and air conditioning in buildings

This system is based on heating the air in a pneumatic solar collector, and then transporting it by a fan to different locations in the house.

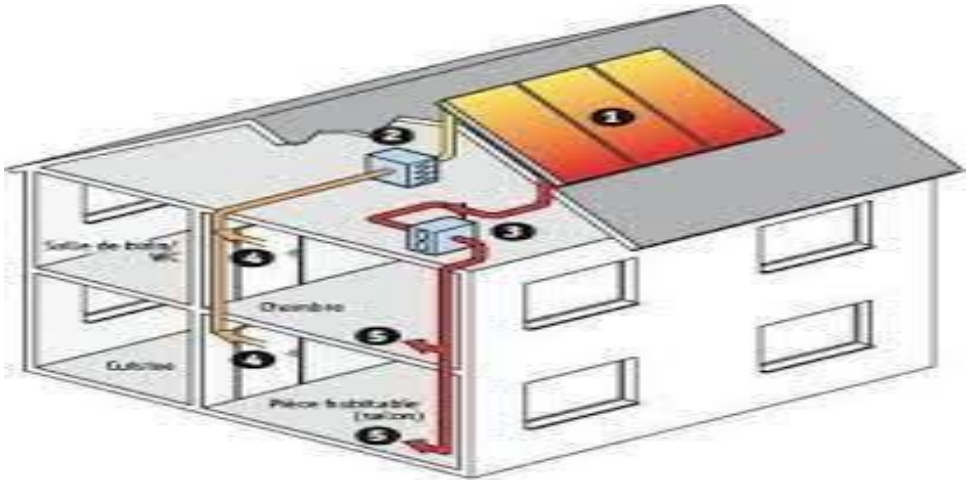

Figure I. 5: Heating and air conditioning of homes [7].

1- Solar collector air plane 2- Filter 3- Fan 4- Air inlets. 5- Air outlets

The goals of Heating, ventilation and air conditioning systems installed inside houses or buildings include thermal comfort for occupants and clean air, saving money and improving the thermal balance of buildings during the middle of the season, especially in the winter period, which leads to improved energy efficiency through the use of modern technologies and the adoption of effective strategies such as air circulation in the building by a control panel., Significant gains can be achieved

The air heating and ventilation systems can create a comfortable and healthy indoor environment while reducing energy consumption [7, 14].

I.3.3.2 Production of mechanical energy

In water-scarce or hard-to-reach areas, such as arid countries and isolated areas, solar energy machines are a promising solution to meet energy, The technology of converting solar energy into mechanical energy is usually used.by the hot air engine, the principle of operation of which is as follows:

The air contained in the atmosphere inside the cylinder is compressed by a piston, the compressed air is heated by an air sensor, which causes it to overheat and expand. the expanding hot air pushes the piston, producing mechanical energy, when the piston returns, the hot air is cooled through a cold source, and then the cold air is compressed again by the piston, and so on [7].

I.3.3.3 Solar drying

The solar drying process is considered one of the most important applications of solar energy, which was used in ancient times for the production of agricultural and food crops. During it, water is extracted from solid or semi-solid liquids by the evaporation process, usually this process is carried out outdoors under direct sunlight.

The drying rate is controlled by external factors, such as solar radiation, ambient temperature, wind speed and relative humidity, as well as internal factors such as the initial water content, product type and mass.

The main purpose of the drying process is to reduce the water content in agricultural food products, reducing the residual values that contribute to the reproduction of microorganisms.

One of the ways to optimize the solar drying process is to use flat solar collectors, where air flows over, under or on both sides of them. This type of system usually optimizes by directing the airflow under the solar panel to reduce heat loss through the glass.

The use of solar collectors for drying crops is an ideal option in such cases as drying tea, coffee, fruits, beans, rice, spices, rubber, cocoa, wood. Figure illustrates this process

illustratively [7, 15, 16].

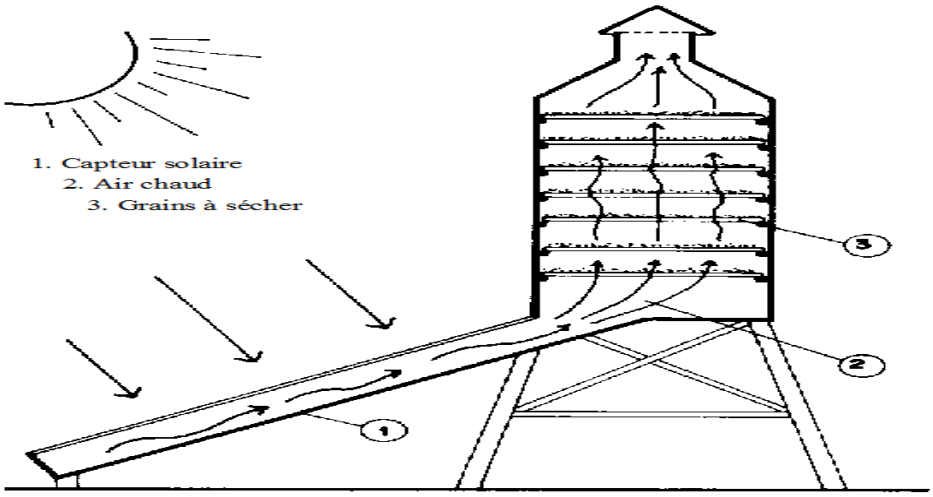

Figure I. 6: Solar drying [7].

I.3.4 Types of solar air collectors

The field of solar collectors is an active field, and to improve the performance of solar collectors, researchers have developed new designs for solar collectors with multiple airflow paths. Among these are the single-pass and double-pass solar collectors.

I.3.4.1 Single-pass solar collectors

SPSAH are the simplest solar collector designs in terms of manufacturing, design and maintenance. They are also the least expensive type of solar collectors. These collectors consist of a single pass that allows air to flow between the glass cover and the absorber plate, where air flows in one direction, either above or below the absorber plate from the air inlet to its outlet as shown in the fig 7.

They are less efficient compared to multi-pass collectors, since the air does not have enough time to effectively absorb heat [17, 18].

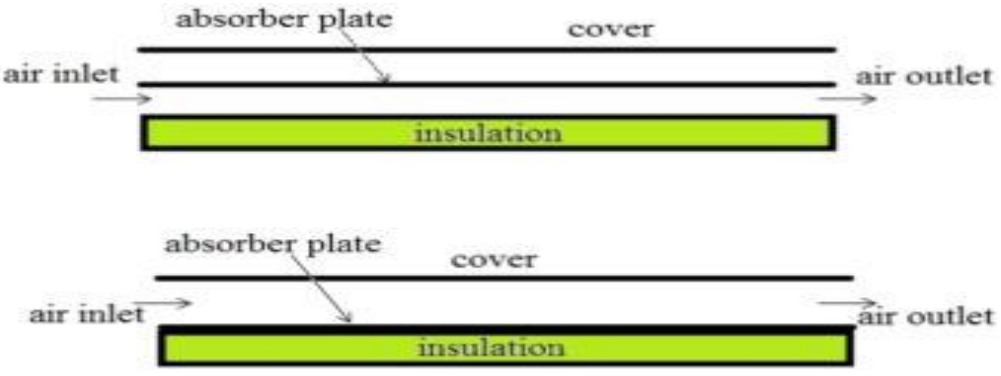

Figure I. 7: Single Pass Solar Air collector [18].

I.3.4.2 Double-pass solar collectors

The concept of a DPSAH was first introduced by Satcunanathan and Devaraj with the aim of reducing heat loss from the bottom and side walls, this design features air flow through two passages that can be opposite or parallel.

In the first pass, the air flows between the glass cover and the absorption plate, where it flows along the upper side of the absorption plate to absorb heat. After that, the air is directed in the opposite direction in the lower pass between the absorber plate and the thermally insulated bottom plate, this allows more heat transferred.

Thanks to the DPSAH, the air can absorb a larger amount of heat, which leads to a higher thermal efficiency of up to 10-15% compared to single-pass designs [18, 19].

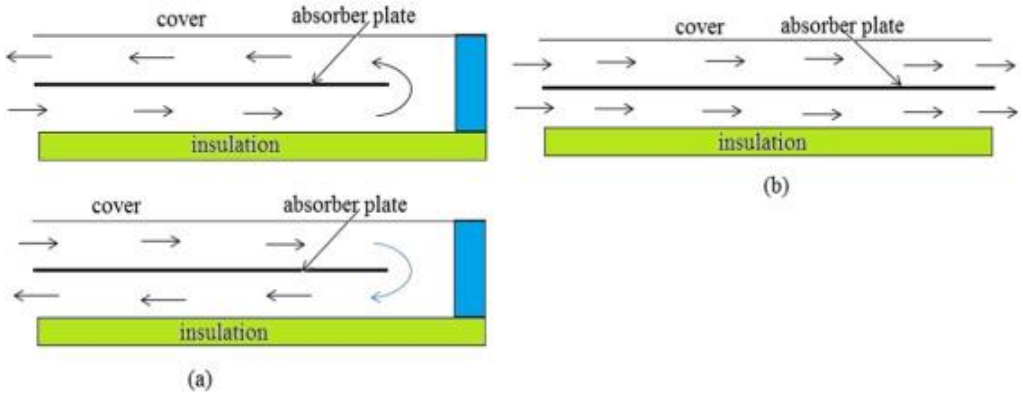

Figure I. 8: Double Pass Solar Air collector (a-counter flow b-parallel flow)[18].

I.4 Conclusion

Through our study of the solar field and SAH, we've realized the significant role that solar collectors can play. This technology relies on harnessing solar energy to heat air, used for heating, cooling, electricity generation, and water heating. SAH are considered a sustainable alternative to fossil fuels, contributing to reducing harmful emissions, improving air quality, achieving energy independence, and lowering energy costs.

In the next chapter, we will discuss a group of previous research that dealt with the topic of a DPSAH.

Chapter II: Literature review

II.1 Introduction

DPSAH are the subject of many existing researches, which can be theoretical, numerical or experimental. The researchers aim to increase the rate of heat transfer between the absorbent plate and the air, and to achieve their goal, they used several techniques to improve the performance of the heat exchangers of the solar collector. These include the use of undulating surfaces, fins and Phase-Change Materials.

Given the pivotal role of current studies in enriching our research endeavors, this chapter serves to provide a comprehensive review of previous research on dual-pass solar air collectors. By pooling ideas from a variety of studies available online, we aim to deepen their understanding of this technology, and to identi. Through this endeavor, we are trying to contribute to the advancement of knowledge in the field of SAH and facilitate the development of more efficient and sustainable energy solutions.

II.2 The importance of previous research on double-pass solar air collectors

Previous studies of the DPSAH are a valuable tool for researchers and designers. They provide a strong knowledge base that provides them with time and effort to start their research. These studies provide information on the various advanced techniques used in the solar aerobic collector study, as well as on its different dimensions and factors affecting its effectiveness. This knowledge is useful for developing and designing more efficient systems, and helps avoid falling into past mistakes.

II.3 Research on double-pass solar air collectors

A summary of the work done on DPSAH, covering theoretical, numerical, and experimental approaches, has been compiled.

Assadeg et al in 2021 [20], scientific research was conducted on the Energetic and exergetic analysis of a new double pass solar air collector with fins and phase change material. The authors conducted numerical analysis using MATLAB and mathematical equations of energy balance were solved by turning the matrix.

The main objective of this research is to study different designs of DPSAH for use in drying applications. These designs include finned and PCM manifesters, with only fins, with

PCM only, without fins and PCM. The results showed that the best-performing designs in terms of energy efficiency were DPSAH equipped with fins and PCM units. The highest efficiency achieved by the proposed complex at a certain air flow rate was 73%. Energy efficiency ranges from 2.5% to 4.2%, The attached fig, clarified by Assadeg et al is schematic diagram of DPSAH with fins and PCM.

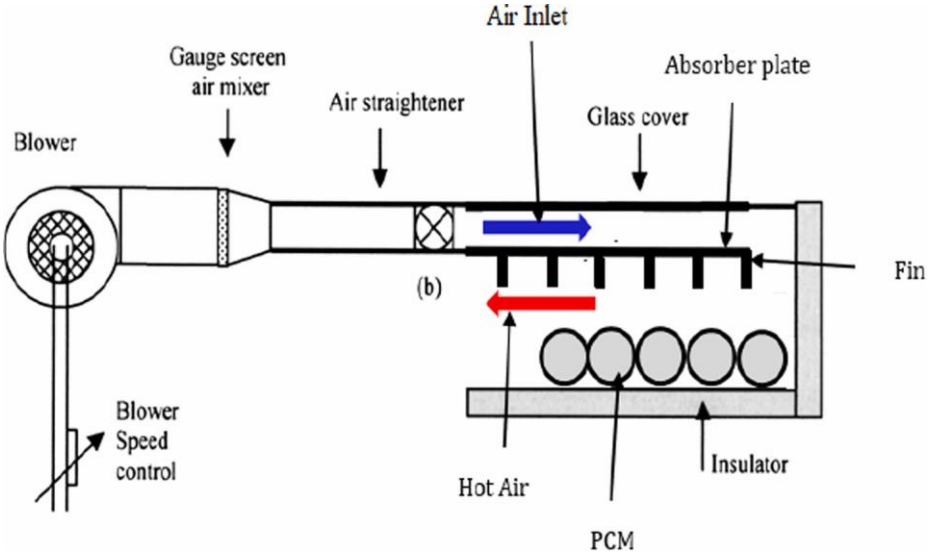

Figure II. 9: schematic diagram of DPSAH with fins and PCM [20].

Belloufi et al in 2023 [21], They published a study about thermal performance of the DPSAH numerical and experimental investigation. The authors conducted experimental and numerical analysis using a mathematical model based on energy balance equations in a system to predict temperature distribution. The study aimed to enhance and develop a theoretical model for estimating the efficiency of DPSAH collectors. It focused on identifying different conditions of mass flow rate (MFR) and solar radiation. By using mathematical equations to calculate the outlet temperature, the researchers analyzed and compared the two models, concluding that solar radiation has a positive effect on DPSAH efficiency, with higher levels leading to greater efficiencies Additionally they found that increasing the length of DPSAH improves its thermal performance, reaching maximum efficiency at L = 9m. The study suggests a significant correlation between experimentally measured values and the results obtained from the proposed method in terms of both quality and quantity.The attached fig, clarified by Belloufi et al is a flowchart outlining a mathematical solution procedure.

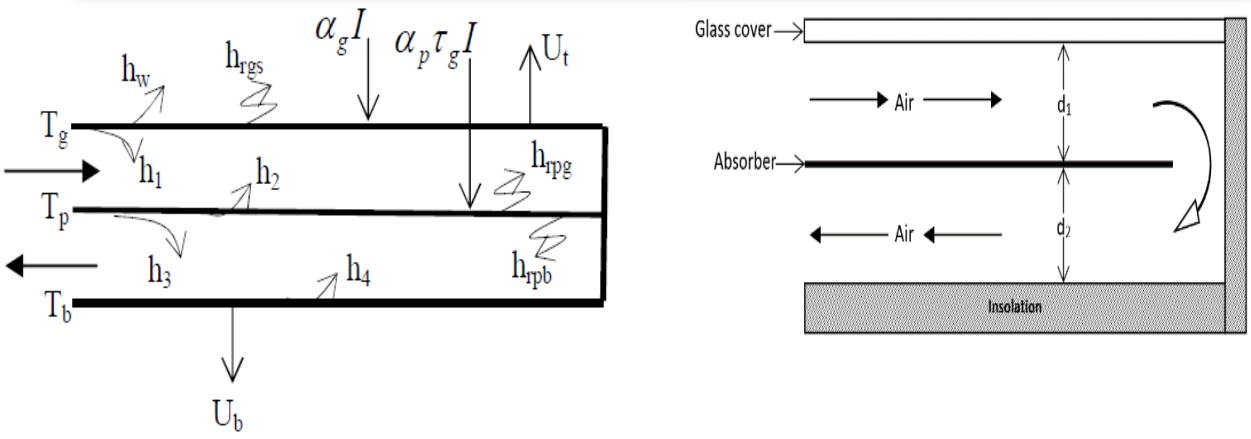

Figure II. 10: Schematic representation of the DPSAH model under study and its heat transfer coefficients [21].

Pramanik et al in 2017 [22], They did a study about Performance analysis of double pass solar air heater with bottom extended Surface. Using an experimental theoretical approach to verify overall output performance compared to initial performance where flow trend is reversed compared to conventional. This study aims to design a solar air heater with a different selective coating model integrated with longitudinal fins at the bottom. Part of the absorbing device is designed to produce hot gases by consuming solar energy in day time. Analyses and results showed an improvement in the efficiency of the complex in solar reverse flow air heaters with an extended surface. Analytical and experimental studies have shown a rise in outside air temperature to acceptable values of up to 69% and 94%, and it has reached its maximum value, which is estimated at 361 K, The attached fig 12, clarified by Pramanik and al is Schematic diagram of a DPSAH.

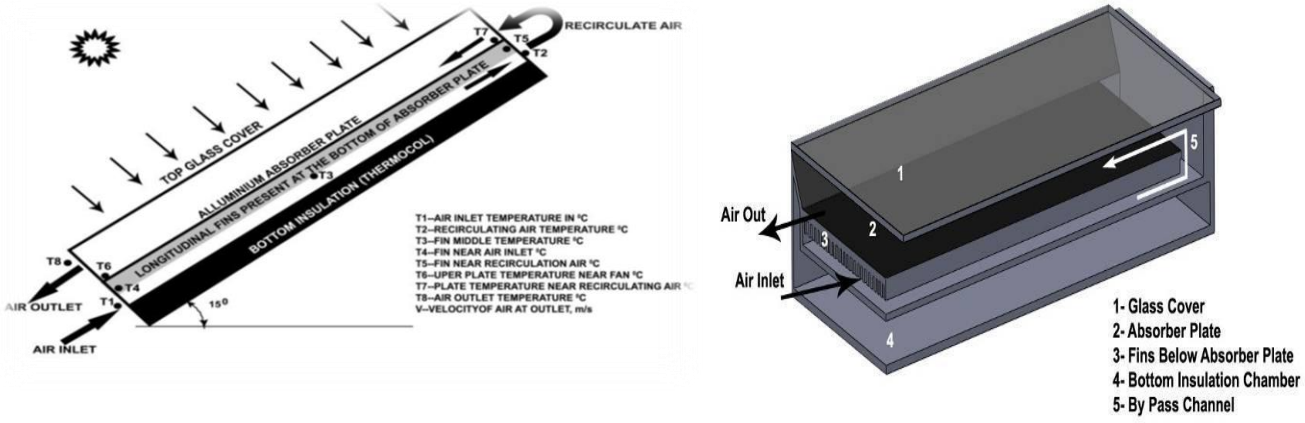

(a) (b)

Figure II. 11: (a) Schematic diagram and (b) Sectional view of a DPSAH with bottom extended surface [22].

Ho et al in (2018) [23], They conducted scientific research on the study Device Performance Improvement of Recycling double-pass cross-corrugated solar air collector and They conducted experimental and theoretical studies on the conditions of recycling and numerically solved them using the Newton method.

The aim of the external recycling collectors is to increase turbulence intensity and expand the heat transfer area as well, to enhance the collector's efficiency. It was observed that there was a significant improvement in heat transfer efficiency using a double-pass recycling device equipped with cross-corrugated absorber plates and Thermal performance was achieved, from which it was concluded that the application of the recycling process on DPSAH is technically and economically feasible and can achieve higher thermal performance compared to both flat panels and fins and baffles attached to solar air collectors; and thermal performance improvements increase with increasing recycling ratio , The attached image, clarified by Ho et al is a schematic drawing of recycling DPSAH.

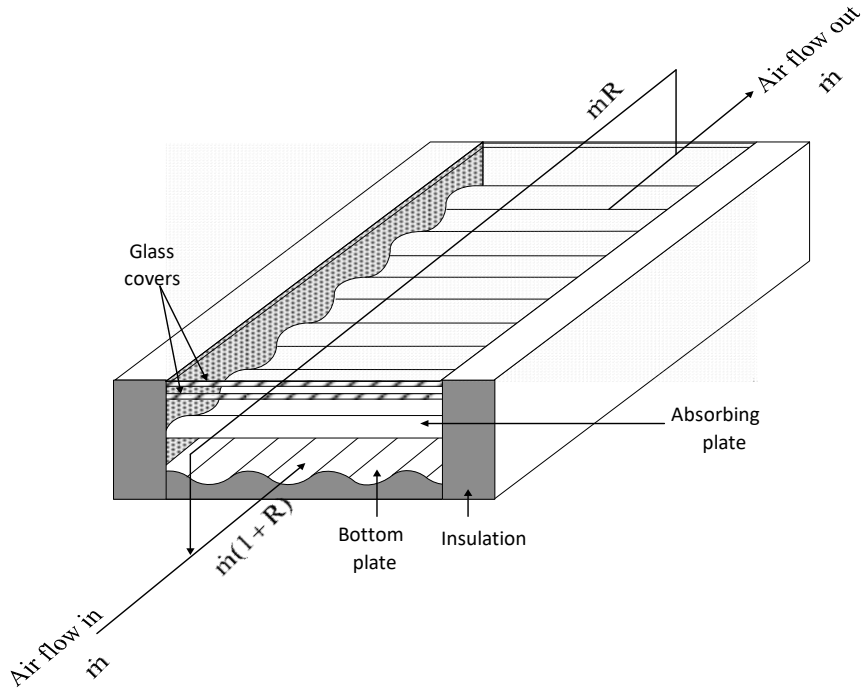

Figure II. 12: A schematic drawing of recycling double-pass cross-corrugated solar air collector [23].

Condorí er in 2023 [24], he conducted scientific research on the study Thermal efficiency characterization of a double-pass parallel flow solar air heater using a quasi-steady model under real operating conditions The objective of this research is to advance the understanding of how solar air collectors perform and to enhance the thermal efficiency of double-pass, parallel-flow solar air collectors using a quasi-steady-state model under actual operating conditions, along with open-loop tests, taking into consideration the heat storage in the absorber plate The

researcher relied on a model based on fixed assumptions about the performance of the complex under changing actual conditions. This study yielded important and diverse results. It found a slight increase in the measured thermal efficiency of the collector, with its average value stabilizing at tilt angles less than 30 °. Additionally, a linear relationship was observed between the temperature difference of the absorber plate and the ambient air validated for a flow rate of 0.19 kg/s with a correlation fit of 98.6%, as well as the temperature difference between the outlet and ambient air. Thermal and hydraulic performance of the collector were evaluated with different flow rates with a maximum of 0.57 for 0.207kg/s, potentially allowing for improvements in the efficiency of double-pass solar air collectors under real conditions, the attached image, clarified by Condorí er is a Stages in the construction of the collector.

Figure II. 13: Stages in the construction of the collector [24].

Kareem et al 2017 [25], They conducted scientific research on Performance analysis of a multi-pass solar thermal collector system under transient state assisted by porous media An experimental study of the MPSAHC system under the transient state in the open field of solar energy was conducted in Petronas University of technology research site, Malaysia, The study aims to achieve the maximum value of the outlet temperature and efficiency of the thermal complex, as the results showed that the hot air supplied by the MPSAHC system reached 70.18 °C, In the middle of the day, while the air produced by the single passage reached 48.53 degrees Celsius and when the double passage reached 57.75 °C and the ambient temperature was 36.64 °C، The maximum efficiency of the thermal Complex reached 72.59% on average daily The

efficiency of the complex was achieved by 36.38% while the energy efficiency ranged from 83% to 67%. This is based on the application of an optimal value of the air mass flow rate, which is estimated at 0.016 kg/s. An extension was observed in the thermal conductivity of the system for a period outside the sun and this is due to the sensory energy stored in the porous media, The attached figure, clarified by Kareem et al see fig 16.

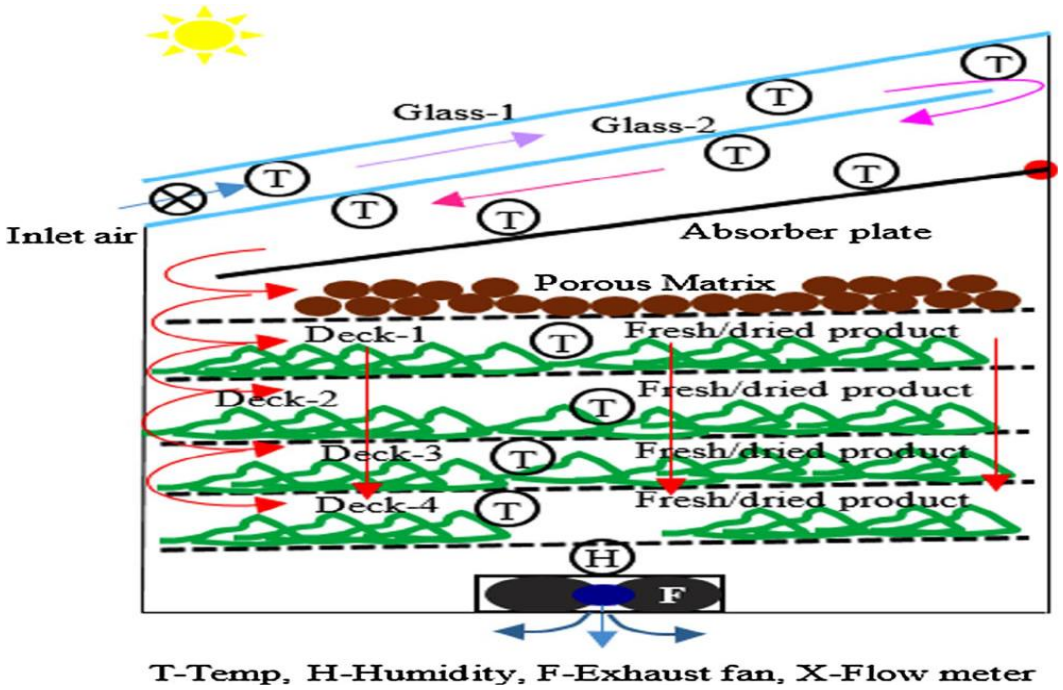

Figure II. 14: Cross section of MPSAHC system test facility [25].

Machi et al in 2022 [26], They did an experimental study about Energy‐based performance analysis of a double pass solar air collector integrated to triangular shaped fins This research is aimed at evaluating the thermal performance of two complexes of the same design, with and without fins. The results showed that the presence of fins in the upper air channels significantly increases both temperatures and the efficiency of the collector. The Daily thermal efficiency of the finned collector was 56.57%, 59.41%, and 61.42%, while for the non-finned collector it was 51.04%, 53.28%, and 57.08% for the mass flow rate of 0.0081, 0.0101, and 0.0121 kg/s.

The thermal efficiency is improved by 4.3-6.1% compared to the non-finned complex. The attached figure, clarified by Machi et al.

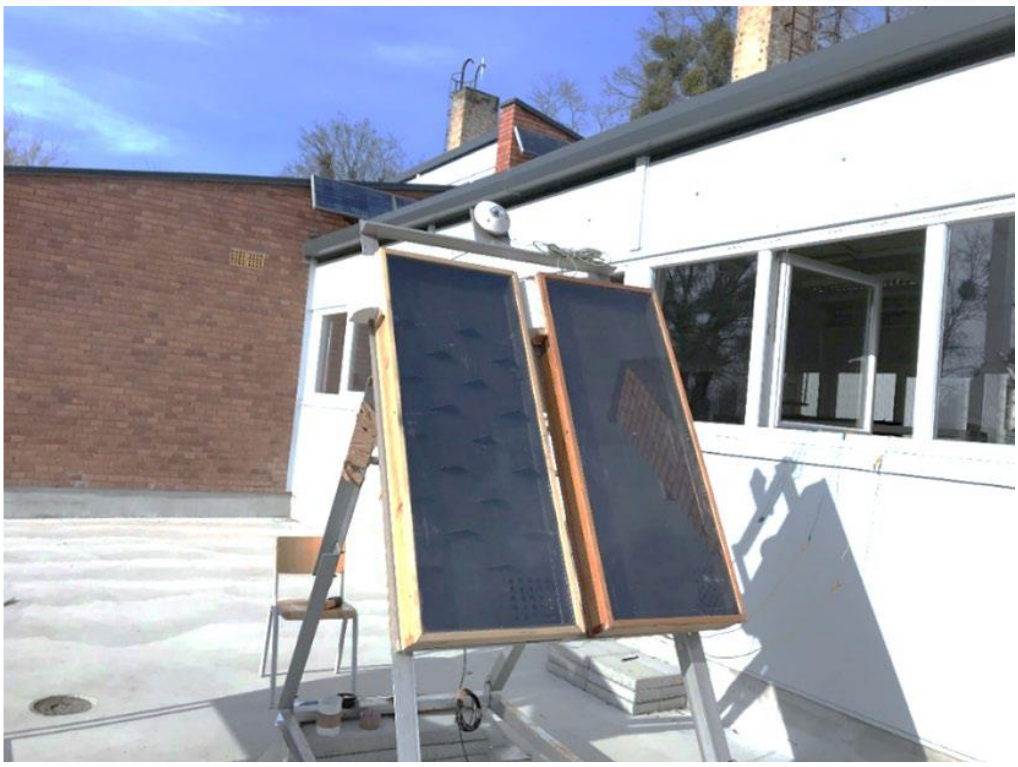

Figure II .15: Testing solar air collectors with and without fins [26].

Salih et al in 2019 [27],they studied the performance of a double-pass solar air heater using multiple rectangular capsules filled with paraffin wax-based on a phase change material PCM . The authors have analyzed experimental and numerical the thermal performance of the DPSAH using multilayered rectangular capsules filled with paraffin wax based on phase change material PCM.

In order to verify the accuracy of these readings, a mathematical model based on finite-volume scheme SIMPLE algorithm was applied to solve the three-dimensional forced convection turbulent flow in the DPSAH. The computational results were in reasonable agreement with the experimental readings. The investigations were carried out at various airflow speed k and three solar irradiance intensities.

The results showed that the increased airflow rate leads to delay in the melting period and decrease melting temperature of the paraffin during the melting period. Furthermore, it can be detected that the optimal discharging period and the air temperature rise of the heater were reached of: 3hr with (17.95e3) C, 2 h with (14e3) C, and 1.25 h with (11e2.5) C.

The attached image, clarified by Salih at al is schematic diagram of (a) Photograph, and (b) outline diagram of an indoor experimental apparatus of the DPSAH integrated with PCM storage unit.

(a) DP-SAH photograph.

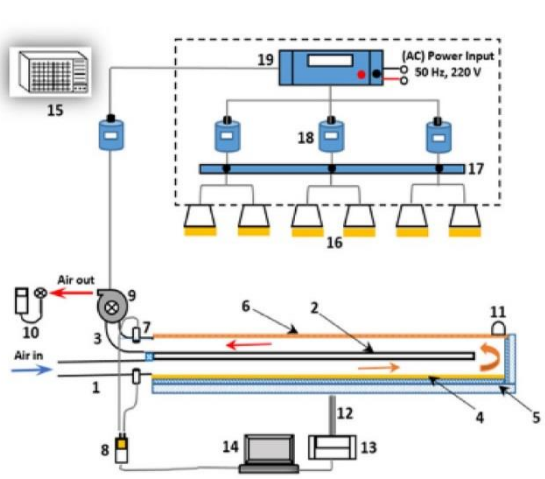

No.	ITEM
1	Inlet duct.
2	Absorber and Container of PCM.
3	Outlet duct.
4	Back plate.
5	Insulation (plywood, glass wool).
6	Glass cover.
7	Pressure taping.
8	Digital manometer.
9	Axial fan.
10	Anemometer (vane type).
11	Solar power meter.
12	Thermocouples wires.
13	Data logger.
14	Laptop.
15	Air conditioner.
16	Halogen lamps.
17	Electrical connector.
18	Contact voltage regulator.
19	Automatic voltage regulator.

(b) Outline diagram.

Figure II.16: (a) Photograph, and (b) outline diagram of an indoor experimental apparatus of the DP-SAH integrated with PCM storage unit[27].

Singh Satyentd er in 2020 [28], he studied the investigations of a single and double pass porous serpentine wavy wire mesh packed bed solar air heater . The author has done an analysis experimental and numerical the thermal performance of a single and double pass porous serpentine wavy wiremesh packed bed solar air heater.

Additionally, numerical simulations using a Computational Fluid Dynamics (CFD) tool were performed and validated against experimental data.

The numerical analysis revealed that the serpentine packed bed solar air heater outperformed the flat packed bed solar air heater by up to 24.33% in terms of thermohydraulic performance.

The experimental results showed that a double pass serpentine packed bed solar air heater with 93% porosity achieved the highest thermal and thermohydraulic efficiencies, approximately 80% and 74%, respectively. This represents an increase of about 18% and 17%

compared to single pass configurations

The attached image, clarified by Singh Satyentde er is schematic diagram of the solar air heater Singh Satyentde .

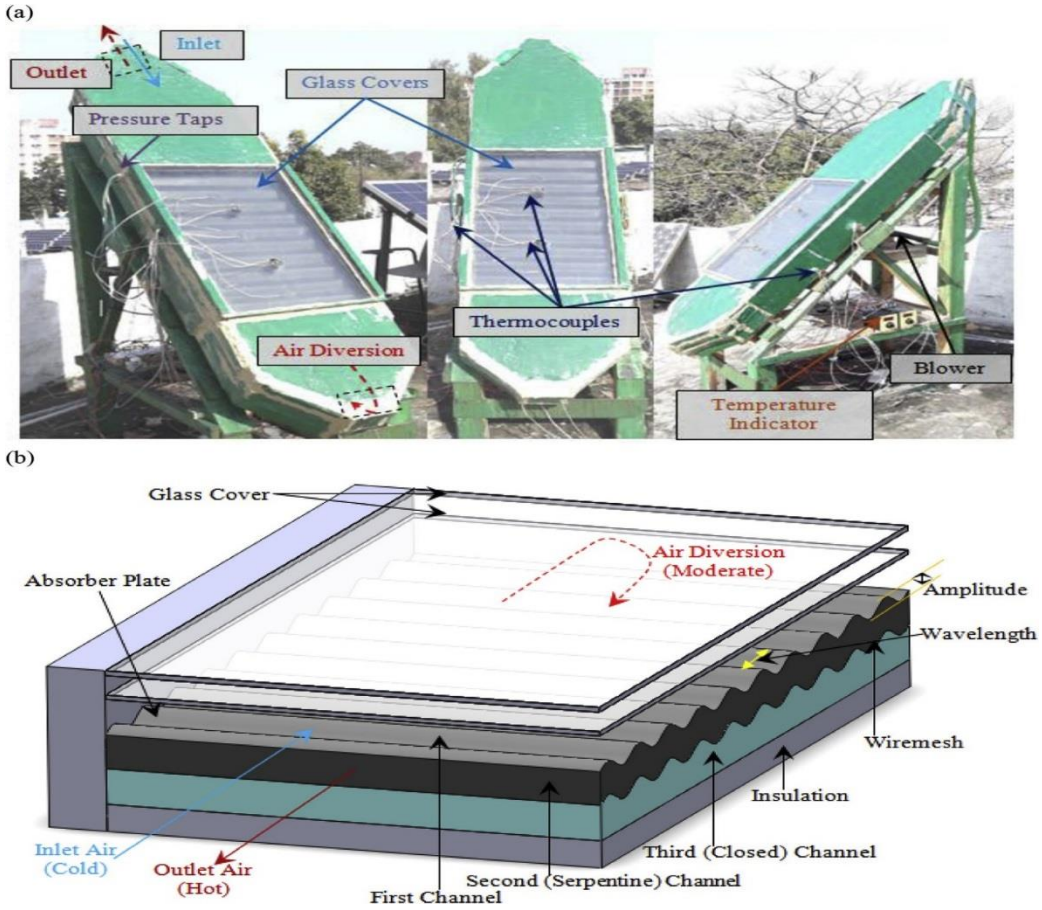

Figure II .17: (a) Actual photographs and (b) schematic of the solar air heaterSingh Satyentde [28].

Sajawal et al in 2019 [29], they studied the Experimental thermal performance analysis of finned tube-phase change material based DPSAH . This experimental study aims to explore the thermal capabilities of a double-pass solar air heater incorporating phase change materials (PCMs) housed within metallic finned tubes, aiming to enhance energy storage and heat transfer rates. The study investigates the charging and discharging characteristics of the PCMs based on experimental findings. Three configurations of the air heater are examined: the first without PCM, the second utilizing RT44HC with a higher melting point in semi-circular finned tubes on the upper pass, and the third combining RT44HC and RT18HC with lower melting points in circular finned tubes on the upper and lower passes, respectively, to augment thermal storage capacity. The thermal performance of each configuration is assessed individually, with results indicating that the third configuration, employing RT44HC and RT18HC in the upper and lower passes, respectively, exhibits the most optimal performance among the tested configurations.

The attached image, clarified by Sajawal et al is schematic diagram of Finned tubes and actual experimental configurations.

Figure II. 18: Finned tubes and actual experimental configurations[29].

El Khadraoui et al in 2017 [30],they studied the Thermal behavior of indirect solar dryer: Nocturnal usage of solar air collector with PCM. The authors have analyzed experimental and numerical the thermal performance of designing, constructing and experimentally studying a forced convection solar dryer using phase change material PCM.

this study explores the viability of employing a solar air heater integrated with Phase Change Material (PCM) for storing solar energy during the day and releasing it at night. The research involved conducting experiments to assess the charging and discharging characteristics of the PCM cavity. Results indicate a daily energy efficiency of 33.9% and a daily exergy efficiency of 8.5% for the solar energy accumulator. Moreover, utilizing the accumulator resulted in maintaining the drying chamber temperature 4 to 16 degrees Celsius higher than ambient temperature throughout the night. Furthermore, the relative humidity in the drying chamber was observed to be 17% to 34.5% lower than ambient relative humidity in the case of the solar dryer with PCM.

The attached image, clarified by El Khadraoui et al is schematic diagram of Photograph of the indirect solar dryer: (1) solar energy accumulator, (2) solar air panel, (3) drying chamber .

Figure II. 19: Photograph of the indirect solar dryer: (1) solar energy accumulator, (2) solar air panel, (3) drying chamber[30].

Wang et al in 2020 [31],they studied the performance of an improved solar air heater with "S" shaped ribs with gap. The authors have analyzed experimental and numerical the thermal performance of improved solar air heater with "S" shaped ribs with gap, where it was done an improved solar air heater design featuring S-shaped ribs with gaps to facilitate improved heat transfer between the air and the heat absorber plate. The design also incorporates gaps within the ribs to reduce air flow resistance. This study presents experimental findings on collector efficiency and pressure drop in the solar air heater equipped with multiple S-shaped ribs with gaps as roughness elements. Various factors affecting rib geometry, such as rib spacing, width, clearance, channel height, solar radiation intensity, and air flow rate, were examined. The study analyzed the impact of these factors on solar air heater heat efficiency and temperature difference between inlet and outlet. Compared to a smooth plate, the solar air heater with artificial roughness demonstrated thermal efficiency improvements ranging from 13% to 48% under different conditions. Importantly, the pressure drop across the new solar air heater remained within a manageable range of 15.8–30 Pa. These experimental results hold significance for the practical implementation of this enhanced solar air heater design.

The attached image, clarified by Wang et al is schematic diagram of Ribs arrangement on collector plate.

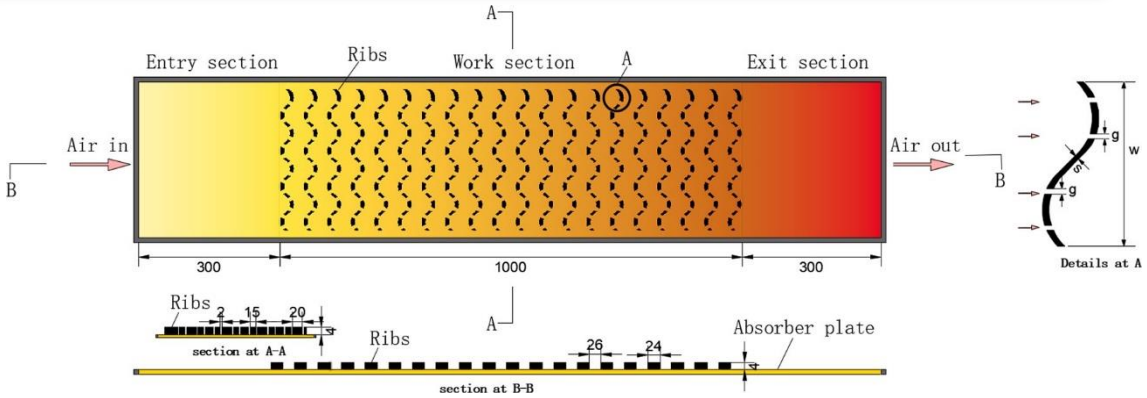

Figure II. 20: Ribs arrangement on collector plate [31].

II.4 Conclusion

This chapter allowed us to review various types of DPSAH, as well as various types of absorbers and factors affecting their efficiency.

The researchers have come to several results that make it possible to optimize various factors that have an impact on thermal efficiency and to exploit the maximum possible energy output from these sensors.

A review of the previous work carried out on this topic also enabled us to take advantage of the work done on DPSAH capacitors, which contributed to the precise definition of the scope of our study within this framework, which targets the single-glass DPSAH thermal complex, which was chosen for its outstanding thermal performance and its ability to adapt and work efficiently within the outlet temperatures ranging from 50 to 100 °C.

Chapter III: Mathematical modeling and numerical simulation

III.1 Introduction

In this chapter, we present a mathematical and numerical model that simulates the flow and transfer of air heat inside the channel of the solar air collector.

The model includes the equations of the transient thermal equilibrium of the five components of the sensor: the window, the liquid in the front phase, the absorber, the liquid in the return phase, and the insulator.

This model is characterized by a deep understanding of the convective and radiant heat exchange mechanisms between each two directly adjacent components, with a special emphasis on he interaction between the absorber ap

ratus and the means of heat transfer. It also provides an overview of the various types of models that have been developed for this purpose, including SPSAH and DPSAH.

III.2 Modeling of the insolator

The thermal balance of an insulator per unit surface area is given by the following equation:

$$I_g = Q_u + Q_p + Q_s \quad (1)$$

Where:

Ig: represents the total incoming heat flux received by the insulated surface.

Qu: refers to the useful energy carried by a heat transfer fluid, such as water or air.

Qp: represents the thermal losses of the surrounding environment through various heat transfer mechanisms, including conduction, convection and radiation.

Qs: The different parts of the insulator.

In the case of steady-state thermal systems and air thermal collectors, the amount of energy stored in the insulation parts is considered negligible, leading to the relationship:

$$I_g = Q_u + Q_p \quad (2)$$

To analyze the temporary behavior of isolated installations and solar collectors, dynamic modeling techniques are used using fictitious discretization in a certain number of steps.

This modeling consists in dividing the catcher into a set of virtual points over a certain number of steps. The equations are obtained by writing the energy equilibria for each point.

The "point-to-point" method of representation consists in dividing the solar collector into virtual segments with a length of "dx" in the direction of the flow of the heat-carrying liquid,

and writing down the energy balance in each segment. It is most appropriate for this purpose to use thermal and electrical analogies [7].

III.2.1 Mathematical modeling of solar panels in steady state

This study aims to analyze the SAH system using the energy balance equations (EBEs). A mathematical model based on the energy balance equations has been developedebes for each component of the SAH system. This study assumes a linear distribution of air temperature inside each component. Then EBEs is used to calculate the average air temperature as follows:

$$Tf = (Tf, i + Tf, o)/2 \quad (3)$$

These equations are considered as the basic tool for the analysis of heat transfer and are appliedon the differential length control volume. This control volume is directed parallel to the flow direction and is located on both the top plate of the glass cover and the absorption plate inside the collector system. Thanks to this model it is possible to evaluate the performance of the complex and its efficiency [21].

III.2.1.1 Simplifying assumptions

With the aim of simplifying the theoretical model, several assumptions have been identified:

- Minimal heat losses from the sidewalls are expected due to their small surface area.
- Neglecting vertical and axial heat conduction it is assumed that heat transfer within each component occurs mainly by convection،
- Each component is represented by only one temperature, rather than representing the temperature gradient within the component.
- It assumes convective heat transfer coefficients, for both external and internal surfaces of the components, constant along the Collector.
- The air flow is supposed to be laminar, represented by an average velocity and any disturbances or eddies in the air flow are ignored.
- Load losses are not taken into account
- The system is supposed to work under steady-state conditions [10, 21].

III.2.1.2 Thermal balance equations for the collectors

The Energy Balance Equations (EBEs) are considered essential for modeling and understanding the behavior of various components within a solar thermal collector system. These equations enable designers to improve the performance of collector components, such as the absorber, glass cover, and heat transfer fluids, ultimately leading to maximizing system

efficiency [21].

III.2.1.3 Modeling of the Single-pass Solar Air Collector

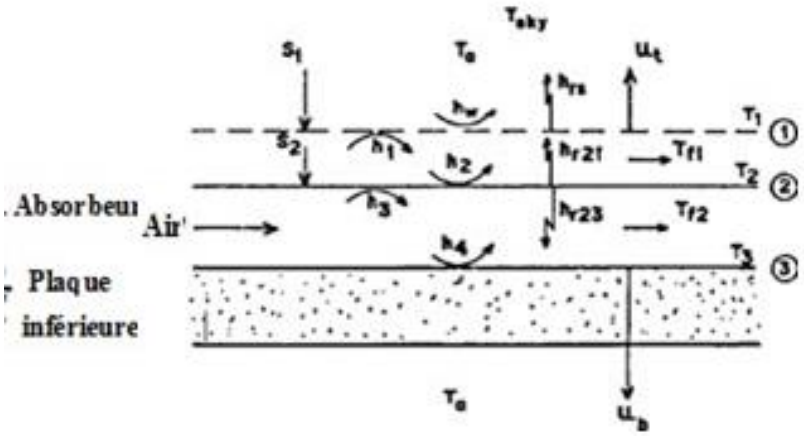

Figure III.21: Schematic Representation of Energy Exchanges of the Single-pass Solar Air Collector[7].

- **Glass cover**

Equation (4) represents the energy balance for the glass cover [7]**.**

$$S_1 + h_{r21}(T_2 - T_1) + h_1(T_2 - T_1) + U_L(T_a - T_1) = 0 \quad (4)$$

$$S_1 = a_1 I_g \quad (5)$$

$$(h_{r21} + h_1 + U_L)T_1 - (h_{r21} + h_1)T_2 = S_1 + U_t T_a$$

- **Absorber**
- Equation (6) represents the energy balance for the absorber [7].

$$h3\,(T2 - Tf) + h1\,(T2 - T1) + hr32\,(T2 - T3) + hr21\,(T2 - T1) = S2 \quad (6$$

$$-(h_1 + h_{r21})T_1 + (h_3 + h_1 + h_{r32} + h_{r21})T_2 - h_3 T_f - h_{r32} T_3 = S_2$$

- **Fluid flowing**

Equation (7) represents the energy balance for the fluid flowing [7].

$$h_1(T1 - T_{f1}) + h_2(T_2 - T_{f1}) = \dot{m}\, Cp \frac{d_{Tf1}}{w\, d_x} \quad (7)$$

$$\Gamma 1(T_{f1,i} - T_{f,i-1}) = h_1(T_1 - T_{f1}) + h_2(T_2 - T_{f1}) \text{ , } \dot{m}\, Cp \frac{d_{Tf1}}{w\, d_x} = \Gamma 1(T_{f1,i} - Tf_{,i-1})$$

$$h_1 T_1 - (h_1 + h_2 + \Gamma_1)T_{f1} + h_2 T_2 = -\Gamma_1 Tf_{,-1}$$

- **Bottom plate**

Equation (8) represents the energy balance for the Bottom plate[7]**.**

$$h_4\,(T_3-T_f)\,dx + U_b\,(T_3-T_a)w\,dx + h_{r32}\,(T_3-T_2)w\,dx = 0 \quad (8)$$

$$-h_{r32}T_2 - h_4T_f + (h_{r32}+U_b+h_4)\,T_3 = U_bT_a$$

III.2.1.4 Resolution method

We used the finite difference method to solve the problem of calculating the glass temperatures, the temperature of the heat transfer fluid, the absorber, and the bottom plate, all of which are functions of time and position.

This method is based on approximating temperature changes using a linear gradient

In each section, the air temperature change is mathematically estimated by the following equation which is known as

$$\frac{dTf}{w\,dx} = \frac{(Tf,i-Tf,i-1)}{w\,dx} \quad (9)$$

$$dA_p = w \times d\,x \quad (10)$$

The system of equations for unknown unknowns T1,T2,Tf, and T3 can be written in matrix form as follows: [A]·[T]=[B]

This system of equations is nonlinear because the matrix [A] and the vector [B] contain coefficients that depend on unknown temperatures [T].

To solve the problem of nonlinearity, an iterative procedure is used. Where at each iteration, the temperatures are calculated using the temperature values from the previous iteration[7].

Equations (4)-(8) above can be presented in 4×4 matrix form

$$[A] = \begin{bmatrix} A_{11} & -(h_{r12}+h_1) & 0 & 0 \\ -(h_1+h_{r12}) & A_{22} & h_3 & -h_{23} \\ 0 & h_3 & A_{33} & h_4 \\ 0 & -h_{r23} & -h_4 & A_{44} \end{bmatrix} [T] = \begin{bmatrix} T_1 \\ T_2 \\ T_{f1} \\ T_3 \end{bmatrix} [B]$$

$$= \begin{bmatrix} S_1 + U_lT_a \\ S_2 \\ -\Gamma 1T_{f2,i-1} \\ UbTa \end{bmatrix}$$

Where:

$$[A_{11}] = [hr21 + h1 + UL\,] \quad (11)$$

$$[A_{22}] = [h_3 + h_1 + hr32 + hr21\,] \quad (12)$$

$$[A_{33}] = -[h_3 + h_4 + \Gamma 1] \quad (13)$$

$$[A_{44}] = [hr32 + Ub + h_4] \quad (14)$$

III.2.1 Modeling of the double pass solar collector

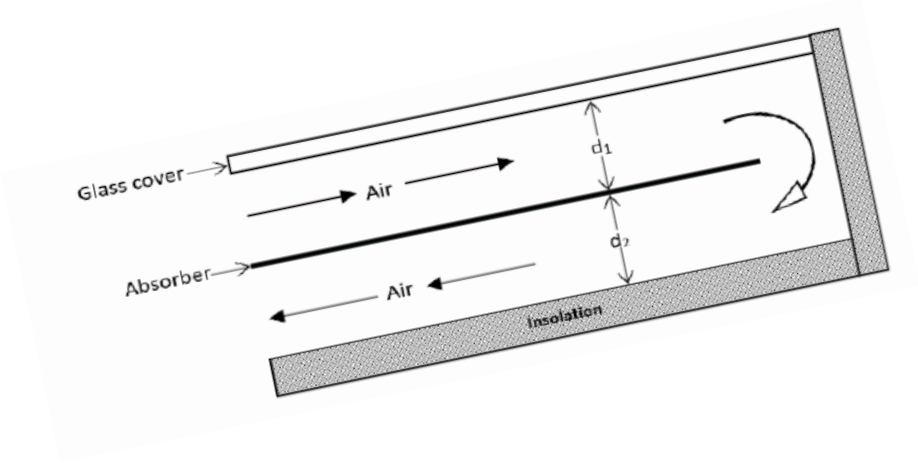

Figure III.22: Schematic representation of the DPSAH model under study[21].

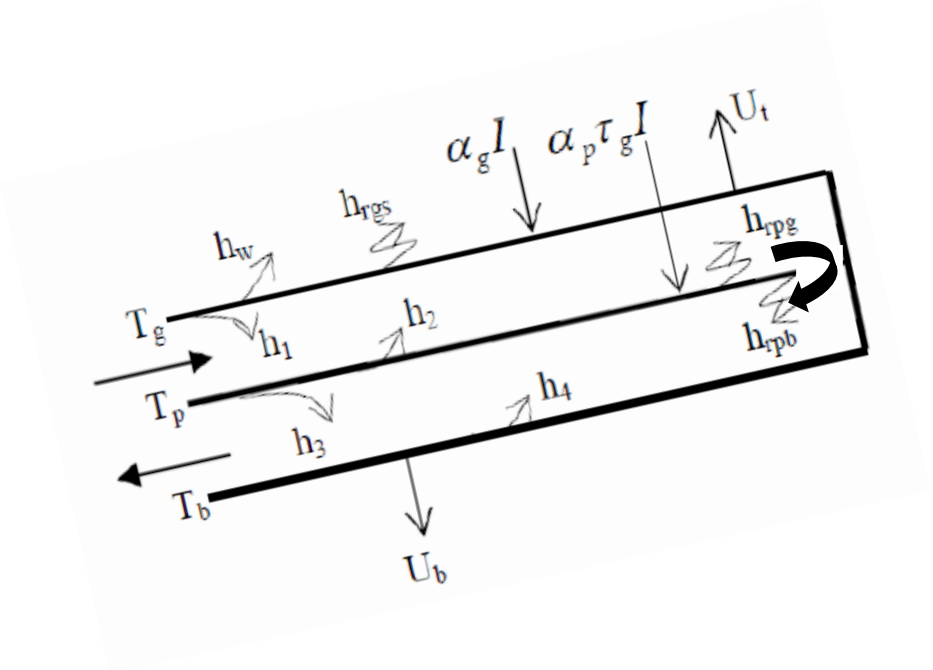

Figure III. 23: Schematic representation of heat transfer coefficients in DPSAH[21].

✓ **Glass cover**

Equation (15) represents the energy balance for the glass cover. It takes into account convection, radiation, and overall heat loss[21].

$$S1 + hr21\,(T2 - T1\,) + h1(Tf1 - T1\,) + UL\,(Ta - T1\,) = 0 \quad (15)$$

$$(hr21 + h1\; +\; UL)\,T1\; - h1Tf1 - hr21T2\; =\; S1 + ULTa$$

Where:

- **The power absorbed by the glass (S1)**

$S_1\; =\; a_1\; I_g$

It takes into account convection h1, radiation hr21, and overall heat loss UL

- **First air flow**

this equation (16) describes the energy balance of the first fluid (f1) flowing in the upper channel by the following equation[21].

$$\dot{m}\; Cp\,\frac{d_{Tf1}}{w\; d_x} = h_1(T1\; - T_{f1}) + h_2(T_2\; - T_{f1}\;) \quad (16)$$

$\mathbf{\Gamma}1(T_{f1,i} - T_{f,i-1}) = h_1(T_1\; - T_{f1}) + h_2(T_2\; - T_{f1})$,

$$\dot{m}\;\mathrm{Cp}\,\frac{\mathrm{d_{Tf1}}}{\mathrm{w\;d_x}} = \mathbf{\Gamma}1(T_{f1,i} - Tf_{,i-1})$$

$$h_1T_1 - (h_1{+}h_2{+}\mathbf{\Gamma}_1)\,T_{f1} + h_2T_2{=}{-}\mathbf{\Gamma}_1Tf_{,-1}$$

It takes into account the $h1$, $h2$ convection, between the glass cover and the fluid in the channel, as well as between the absorption plate and the fluid in the channel, As well as $\dot{m}$ and Cp are respectively the mass flow rate of the liquid in the channel, and the specific heat capacity

- **Absorber plate**

The energy balance for the absorber is expressed by the following equation[21].

$$h2\;(T2\; - Tf1\;)\; +\; h3\;(T2\; - Tf1\;)\; +\; hr21\;(T2\; - T1\;) + \quad (17)$$
$$hr32\;(T2\; - T3\;) =\; S2$$

$$-hr21\;T1\; -\; (h3 + h3)Tf1 +\; (h2 + h3\; +\; hr32\; +\; hr21\;)\,T2 - hr32T3 = S2$$

Where:

- **Power absorbed by the absorber ($S2$)**

$S2 = \tau\alpha 2Ig$

α2 is the absorber absorption coefficient and τ is the glass transmittance.

- **Second air flow**

this equation describes the energy balance of the second fluid (f2) flowing in the lower channel by the following equation[21].

$$\dot{m}\; Cp\,\frac{d_{Tf2}}{w\; d_x} = h3(T2\; - Tf2) + h4(T3\; - Tf2\;) \quad (18)$$

$$\Gamma 2(\mathrm{Tf2,i}\; -\; \mathrm{Tf2,i} - 1)\; =\; \mathrm{h3(T2}\; -\; \mathrm{Tf}\,) +\; \mathrm{h4(T3}\; -\; \mathrm{Tf}\,)$$

$$\dot{m}\ Cp\frac{d_{Tf2}}{w\ d_x} = = \mathbf{\Gamma}2(Tf,i - Tf,i{-}1)$$

$$h3T2\ -\ (h3 + h4 + \Gamma 1)\ Tf2,i\ +\ h4T3 = -\Gamma 2Tf2,i - 1$$

In the equation (18), h3 is the convective heat transfer coefficient between absorber plate and air flow and h4 represents the convective heat transfer coefficient between bottom plate

- **Bottom plate**

the energy balance for the insulation is given by the following [21].

$$h4\ (T3 - Tf\ )\ + Ub\ (T3 - Ta) + hr32\ (T3\ -\ T2)\ =\ 0 \qquad (19)$$

$$-hr32T2 - h4Tf2 + (hr32 + Ub\ +\ h4)\ T3\ = UbTa$$

Where:

Ub is the overall thermal loss coefficient and hr32 is the radiation heat transfer coefficient between bottom plate and absorber plate.

$$[A] = \begin{bmatrix} A_{11} & -h_1 & -h_{r12} & 0 & 0 \\ h_1 & A_{22} & h_2 & 0 & 0 \\ -h_{r21} & -h_2 & A_{33} & -h_3 & -h_{r23} \\ 0 & 0 & h_3 & A_{44} & h_4 \\ 0 & 0 & -h_{r23} & -h_4 & A_{55} \end{bmatrix} [T] = \begin{bmatrix} T_1 \\ T_{f1} \\ T_2 \\ T_{f2} \\ T_3 \end{bmatrix}$$

$$\text{And } [B] = \begin{bmatrix} S_1 + U_l T_a \\ - \quad \Gamma 1 \ T_{f,i-1} \\ \vdots \quad S_2 \quad \vdots \\ - \quad \Gamma 2 \ T_{f2,i-1} \\ U_b \quad T_a \quad \vdots \end{bmatrix}$$

Where:

$$[A_{11}] = [hr21 + h1\ +\ UL\ ] \qquad (20)$$

$$[A_{22}] = -[h_1 + h_2 + \Gamma 1\ ] \qquad (21)$$

$$[A_{33}] = [h_2 + h_3\ +\ hr32\ +\ hr21\ ] \qquad (22)$$

$$[A_{44}] = -[h_3 + h_4 + \Gamma 1] \qquad (23)$$

$$[A_{55}] = [hr32 + Ub\ + h_4\ ] \qquad (24)$$

III.3 Approximating the coefficients of heat transfer

Heat transfer coefficients are used to describe how heat is transferred between two surfaces or mediums. These coefficients can be estimated using a variety of methods, depending on the particular application and the type of heat transfer mechanism involved. The choice of the method used to estimate the heat transfer coefficient depends on the specific application and available resources[21].

III.3.1 Influence of air currents

- The convective heat transfer coefficient between the air and the absorber plate

Is obtained using equations (25) and (26) are used, respectively, to get The convective heat transfer coefficient of the air flowing through the channel under laminar flow can be estimated by the following relation [7, 21]:

If Re < 2300

$$Nu = \frac{h3\ Dh}{kf} = \frac{4.4+0.00398(0.7ReDh/L)^{1.66}}{1+0.0114(0.7ReDh/L)^{1.12}} \quad (25)$$

And for fully developed turbulent flow, the heat transfer coefficient is calculated by:

If Re > 2300

$$Nu = \frac{h3\ Dh}{kf} = 0.0158\ Re^{0.8} \quad (26)$$

III.3.1.1 Radiative transfer

- between the sky and the cover glass

The radiation heat transfer coefficient between the sky and the glass is given by the following expression:

$$hrs = \sigma s1(T1 + Ts)(T2 + T2)(T1 - Ts)/(T1 - Ta) \quad (27)$$

With

σ as the Stefan-Boltzmann constant (σ = 5.673×10^{-8} W/m^2·K^4).

T_1 as the temperature of the glass,

Ts is the equivalent temperature of the celestial dome, and it can be determined using the following formula:

$$Ts = 0{,}0552.Ta^{1.5} \quad (28)$$

The temperatures Ts and Ta are expressed in Kelvin.

- between the absorber plate and the cover glass:)

$$hr21 = \frac{\sigma(T1^2 + T2^2)(T1 + T2)}{\frac{1}{\varepsilon_1} + \frac{1}{\varepsilon_2} - 1} \quad (29)$$

The temperatures T_1 and T_2 are expressed in Kelvin.

- between the absorber and the lower plate.

$$hr23 = \frac{\sigma(T2^2 + T3^2)(T2 + T3)}{\frac{1}{\varepsilon_2} + \frac{1}{\varepsilon_3} - 1} \quad (30)$$

The temperatures T_2 and T_3 are expressed in Kelvin.

III. 3.1.2 Convective transfer

- Convective transfer due to wind

Heat transfer coefficient of wind:

$$hw = 5{,}67 + 3{,}86\,Vv \quad (31)$$

- Convective transfers in the sensor

Equation (14) can be used to determine the coefficient of radiative heat transfer between the cover glass and the absorption plate:

$$h1 = 1.42\left(\frac{(T2 + Ta)\,sin\beta}{L}\right)^{1/4} \quad (32)$$

The temperatures T_2 and T_a are expressed in Kelvin.

Where:

$$h_1 = h_2 \quad (33)$$

h_2 between absorber plate and air flow

- In the mobile air stream

In the context of forced convection, and for rectangular ducts, the exchange between the absorber and the heat transfer fluid is characterized by the coefficient:

$$h3 = \frac{Nu\,D_h}{k_f} \quad (34)$$

Where:

$$h_3 = h_4 \quad (35)$$

III. 3.1.3 Thermal losses

The coefficient of thermal heat loss towards the back of the solar air heater can be calculated using the equation:

$$Ub = \frac{1}{i=\sum_1^n \frac{Xbi}{kbi} + \frac{1}{hw}} \quad (36)$$

Where:

kbi Thermal conductivity of insulation

Xbi Insulation thickness

The coefficient of thermal heat loss for the air in front of the solar air heater is expressed as:

$$UL = hrs + hw \quad (37)$$

Where:

hw is the convective heat transfer coefficient due to wind, between the underside of the insulator and the outdoor air.

III.3.2 Proprieties of air flow

The following expressions are utilized to depict the fluctuating thermal characteristics of air [21]:

$$Cp = 999.2 + 0.143Tf + 1.61 \times 10^{-4}\, Tf^{\,2} - 6.75 \times 10^{-8}\, Tf^3 \quad (38)$$

$$K = 0.0244 + 0.6773 \times 10^{-4} Tf \quad (39)$$

$$\upsilon = 0.12844 \times 10^{-4} + 0.00105 \times 10^{-4} Tf \quad (40)$$

$$\rho = \frac{353.44}{Tf + 273.15} \quad (41)$$

The air temperature, evaluated in Celsius, can be denoted as T_f.

Where:

The density ρ, thermal conductivity k, and dynamic v viscosity μ of the air

III.3.3 Thermal efficiency and useful energy (recovered by the heat transfer fluid)

Given that the inlet and outlet air temperatures are known, the following equation can be used to represent the useful energy[7]:

$$Qu = m^{\cdot}\, Cp(Tfs - Tfi) \quad (42)$$

the thermal efficiency ɳ of the collector can be calculated by:

$$ɳ = \frac{Qu}{I_g A_p} \quad (43)$$

III.4 Conclusion

In this chapter, energy balance equations were presented to derive the steady-state solution. These equations were applied to each component of the solar air collector, considering the simplified assumptions we made. We then developed a program using "MATLAB", which enabled us to calculate the thermal performance of flat-plate solar collectors whether single-pass or double-pass.

Subsequently, the results obtained in both cases will be compared with experimental results to validate the model overall.

Chapter IV : results and discussions

IV.1 Introduction

In this chapter we will present and verify the most important results obtained from numerical models related to the DPSAH, with the experimental data of previous studies. The main results will be presented and analyzed in the form of curves and graphs to facilitate understanding and interpretation of the performance of these systems under various operating conditions.

IV.2 Parametric study

The table (2) contains a set of operational data of a DPSAH, which describe the operating conditions and characteristics of a solar thermal collector system used in the code.

Table Ⅳ. 2: Table representing the operational data of a DPSAH for our code.

parametric	Symbols	Values	Unit
Incident solar radiation	Ig	1000	(W/m^2)
Wind speed	V	2.4	(m/s)
Heat capacity of air	Cp	1012	(J/Kg K)
Air mass flow rate	$\dot{m}$	0.01	(Kg/s)
Angle of inclination of the collector	A	30	degree
Length of collector	L	2	(m)
Width	W	1	(m)
Ambient temperature	T_a	25	(C)

IV.3 Validation of results

IV.3.1 Validations with literature

The numerical model has been validated by previous research conducted by fudhli et al and belloufi et al[21, 32].

- **Double pass solar air collector**

We compared and analyzed the experimental results presented by Futholi et al [32] ,and others with the results obtained from our numerical model under the same operating conditions (Ig = 425 W/m^2, and variable air flow).

Figure 24 Outlet temperature as a function of mass flow rate and system properties. And illustrates the evaluation of the performance of the current model, flowing at the same rate as experiment the Futholi et al [32]. The current results indicate that our numerical results positively agree with the experimental results of Futholi et al [32], with the highest error rate recorded at 4.77%.

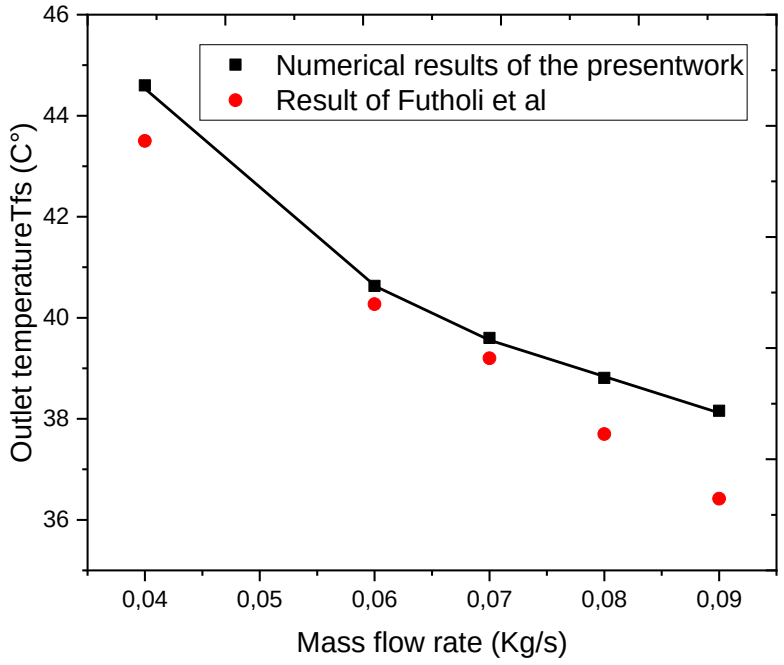

Figure Ⅳ. 24: Variation of the outlet temperature as a function of mass flow rate.

Table Ⅳ.3. The outlet temperature of the DPSAH at different incident solar radiation and different mass flow rates (validation of the numerical model with Futholi et al[32].)

Ig(W/m^2)	Mass flow rate (Kg/s)	Outlet temperature (°C)		
		Present result	Result of Futholi et al [32].	Error %
425	0.04	44.60	43.5	2.52
	0.06	40.63	40.27	0.89

	0.07	39.6	39.2	1.02
	0.08	38.81	37.7	2.94
	0.09	38.16	36.42	4.77

Our numerical results of the air temperature at the outlet DPSAH were compared with the experimental results of Belloufi et al [21], under the same operating conditions (Ig = 790 W/m^2, $\dot{m}$=0.013(Kg/s)). As shown in Table 2, and it seems from this comparison that the performance of the current model follows the same direction as the experimental results، The Maximum error rate was 5.4% and the minimum error rate was 0.02%.

Table Ⅳ. 4. The DPSAH's thermal performance and outlet temperature at different collector length (validation of numerical model with belloufi et al[21].

Length collector (m)	**Outlet temperature (K)**		
	Present result	Result of Belloufi et al	Error%
0	306	306	0
0.77	313.6	331.5	5.4
1.6	321.8	339	5.07
2	325.56	341.5	4.6
1.6	352.7	350.5	0.28
1.77	354.6	357.5	0.8
0	357.22	357.25	0.02

IV.3.2 Outlet Temperature of Components

The curve (25) shows the effect of the length of the solar collector on the outlet temperature at a solar radiation of (Ig=1000W/m2) and a mass flow rate of m=0.01 Kg/s.

We note that the temperature of the first air increases with the length of the DPSAH up to a certain point and this is offset by an increase in the air's absorption of heat in the second pass. This is due to the increased area of heat transfer to the air.

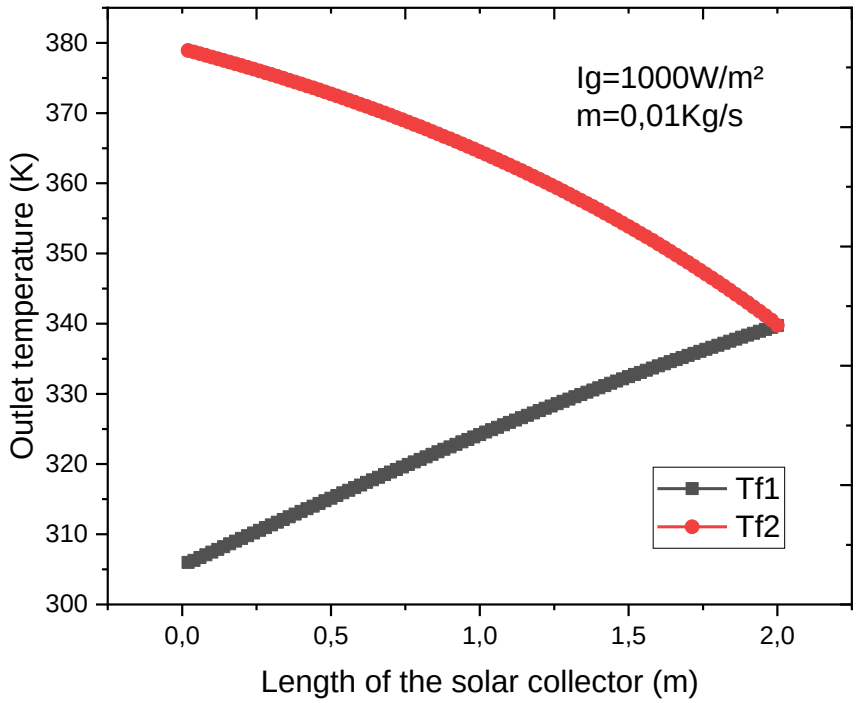

Figure IV. 25: Evolution of the air temperature in relation to the DPSAH length.

In this section, a numerical study was conducted to explore the changes in and temperature of the components of the DPSAH. From Figure 26 it is possible to observe the temperatures of the three different components (glass, absorber, bottom plate) at a constant mass flow rate

(m= 0.01 kg/s) and solar radiation (Ig = 1000 W / m^2). The curve indicates a gradual increase in temperature for all three components as the length of the Collector element increases. This is due to the influence of the initial temperature on the temperature of the components, which leads to a decrease in its value at the beginning of the length of the compound.

- Absorbent: it shows the highest temperature among the three materials due to the low heat loss in it, which leads to heat retention inside the element.
- Bottom plate: it is characterized by a higher temperature compared to glass due to moderate thermal loss.
- Glass: displays the lowest temperature among the three materials due to the high thermal loss in it.

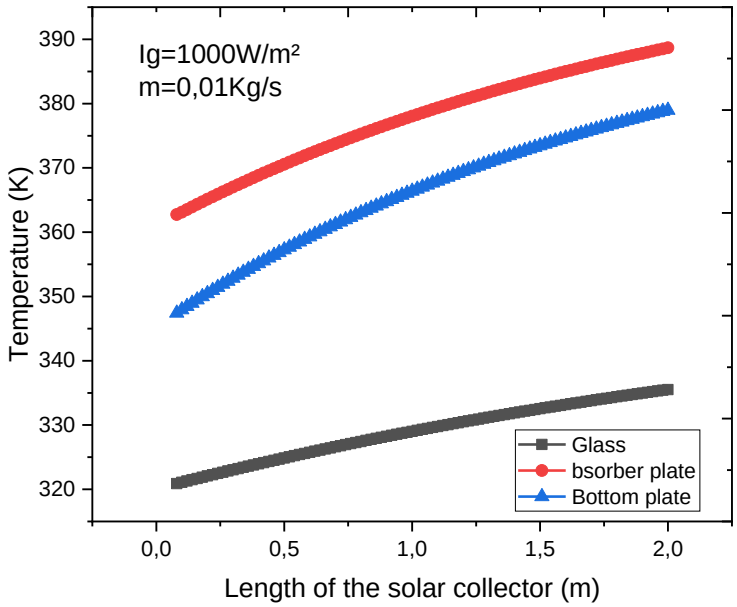

Figure Ⅳ. 26: Variation in the collector elements temperatures according to their length for m=0.01kg/s, Ig=1000w/m^2(Glass, absorber, bottom plate).

IV.3.3 Variation of the outlet temperature as a function of mass flow rate

The curve in Figure 27 shows the change in the outlet temperature as a function of the mass flow at a constant solar radiation value (Ig = 1000 W/m^2). It is noted that a gradual increase in the mass air flow results in a decrease in the outlet temperature.

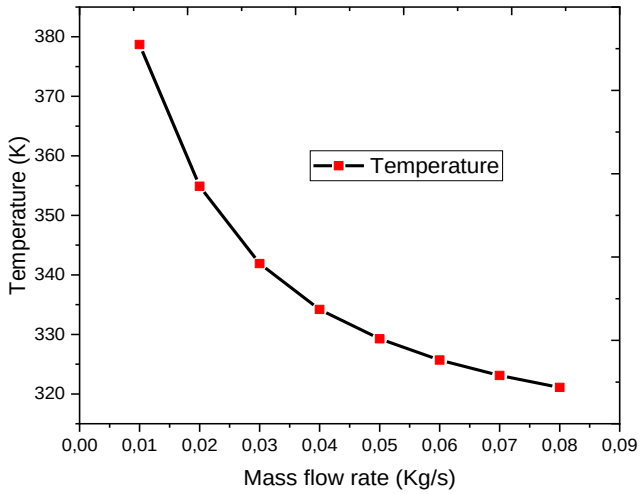

FigurⅣ. 27: Variation of the outlet temperature as a function of mass flow rate

The curve 28 illustrates that the system efficiency decreases with an increase in the mass flow rate. At a low mass flow rate (0.01 kg/s), the efficiency is approximately 88.2%. With an

increase in the mass flow rate to (0.02 kg/s), the efficiency decreases to around 74.6%. Further increase in mass flow rate (0.03 kg/s) results in a reduction in efficiency to about 62.67%.

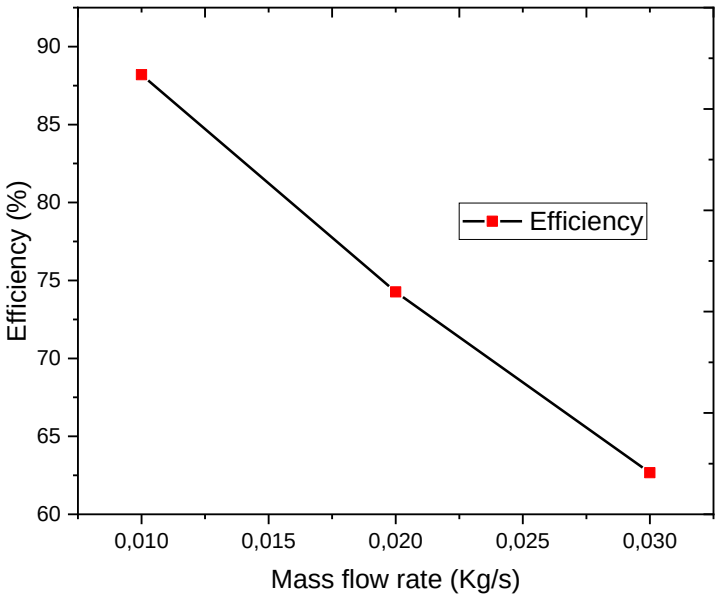

FigureⅣ. 28: Variation of the efficiency as a function of mass flow rate

The curve in Figure 29 hows the variation of the outlet temperature as function of the length of DPSAH (Ig = 1000 W/m^2 and $\dot{m}$=0.01Kg/s).

illustrates that an increase in the length of the solar collector leads to an increase in the surface area exposed to solar radiation, resulting in enhanced heat exchange and an elevation in outlet temperature. However, with a greater increase in length, the rate of temperature rise slows down due to increased heat loss or reaching the thermal efficiency limits of the system.

The displayed curve (Figure 30) depicts the relationship between the air temperature inside the solar collector and its length. There are three curves representing different lengths of the collector (0.5 m, 1 m, 2 m). The x-axis represents the length of the collector (m), while the y-axis represents the outlet air temperature (K). An increase in air temperature with the collector's length was observed, as all curves show a general rise in the air temperature inside the collector with increasing length.

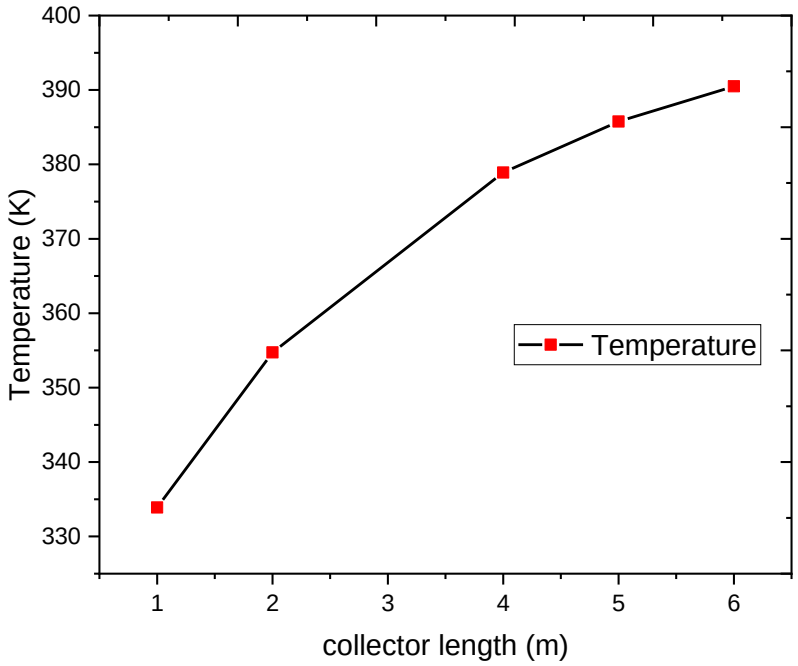

FigureIV. 29: Variation of the outlet temperature as function of the length.

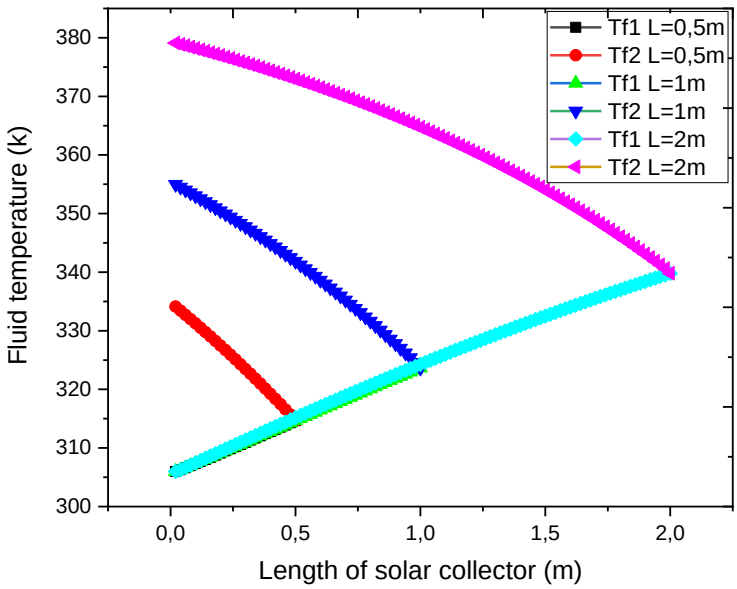

Figure IV. 30: Evolution the air temperature as function of collector's length (0.5m, 1m and 2m).

The curve (31) shows the relationship between solar radiation (W/m²) and outlet temperature (K). There are three data points at solar radiation levels. It is observed that as solar radiation increases, the outlet temperature also increases. The relationship between solar radiation and outlet temperature appears to be nearly linear, with the data points forming an

almost straight line. This indicates that an increase in solar radiation leads to an increase in outlet temperature at an approximately constant rate. This can be explained by the system absorbing more solar energy as radiation increases, resulting in a higher outlet air temperature.

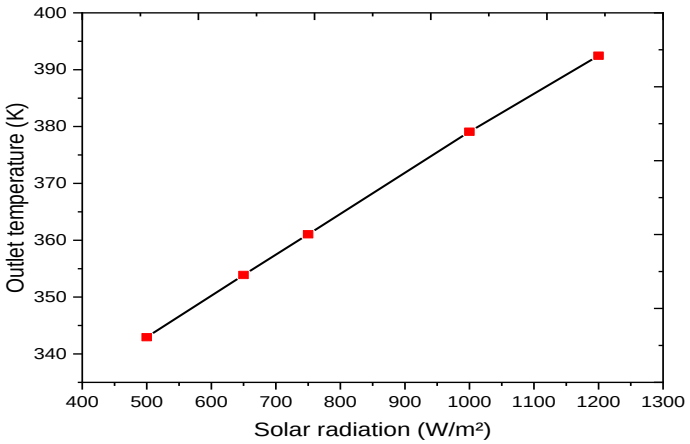

Figure Ⅳ.31: Evolution of the outlet temperature as function of solar radiation

Curve (32) shows the change in air temperature inside (DPSAH) relative to the ambient temperature. This study aims to understand the influence of external environmental conditions, where we observe that there is a direct relationship between them, where the higher the ambient temperature, the higher the outlet temperature.

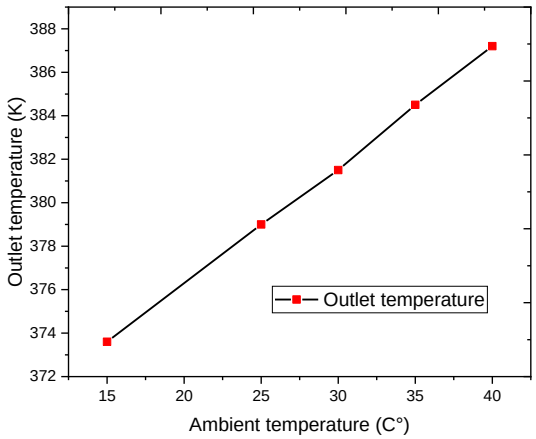

Figure Ⅳ.32: Evolution of outlet temperature relative to ambient temperature for the DPSAH.

IV.3.4 Comparaison between single and double pass collectors

Curve (33) compares a SPSAH and a DPSAH with a length of (2 m).

- SPSAH: the temperature of the liquid rises continuously with the length of

the Collector, which indicates a high efficiency in absorbing and converting solar energy into heat.

- DPSAH: The first passage (Tf1): shows an increase in temperature with the length of the collector, the air was transferred to the second passage (Tf2) to continue absorbing and increasing heat until the exit.

We note that the highest output temperature was recorded in SPSAH. From it we conclude that SPSAH are usually better than double-pass collectors in terms of thermal efficiency and outlet temperature. This is because individual pass collectors have less heat loss.

.

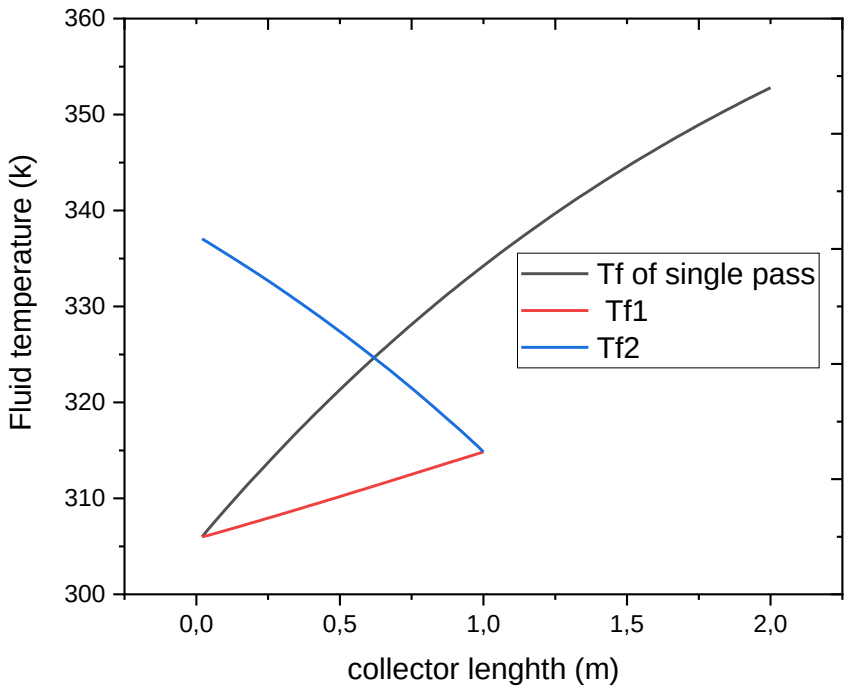

Figure Ⅳ.33: Comparison between single and double pass collectors at the same length of heat transfer.

In the figure 34, we compared between a DPSAH and a SPSAH under the same conditions (Ig = 1000 W/m^2 and $\dot{m}$=0.01Kg/s) and at the same collector length L=2m, where we notice that the outlet temperature in the double-pass is better than the single-pass, as the largest outlet temperature reached 378.9182 K. and in the single-pass it reached 352.7972 K, and this is due to the increase in the heat transfer area.

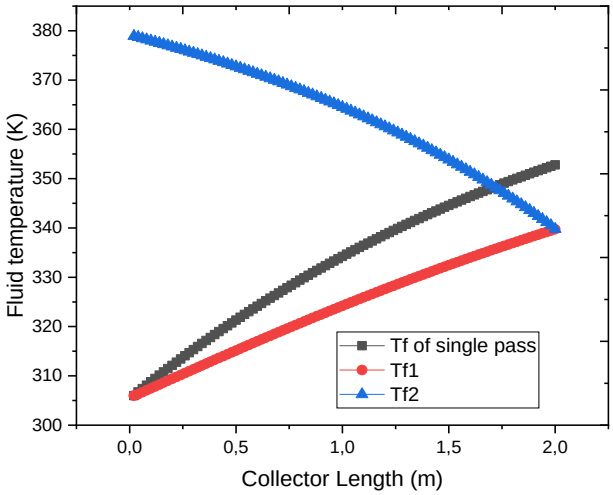

Figure Ⅳ.34: Comparison between single and double pass collectors for the same length(2m) of collector.

Ⅳ.4 Conclusion

This chapter allows to view and verify the results of numerical models and thermal performance analysis of a double-pass solar air heater. The results of the model were compared with the results of previous studies in the same field for accuracy and determined the influence of various factors on the performance of the DPSAH. The main results havebeen presented in the form of graphs and tables to provide a clear and concise picture of the results.

General conclusion

General conclusion

This study provides a numerical analysis of the thermal efficiency of a DPSAH using MATLAB program to evaluate its performance and efficiency. The main objective of the study is to contribute to understanding the heat exchange mechanisms in solar air collection systems under stable conditions.
Firstly, a brief literature review was provided on available works in the literature regarding the thermal perspective of individual and DPSAH. The focus of this study was on previous research, particularly the theoretical aspects.

Subsequently, numerical models used to simulate heat transfer in single and DPSAH sensors were presented. The EBEs were applied to extract the solution of the stability state to control the problem studied. The collector was divided into differential elements to determine the temperature for each component of the collector.

For that, a numerical model, based on the finite difference method, was developed to solve a set of equations derived from a detailed physical model.
The model takes into account the specific thermophysical properties of various elements DPSAH, including glass, absorber, insulation, channels.

The model was validated by a series of experiments that showed accurate results that corresponded to experimental data of belloufi et al [21], we recorded the highest error percentage at 5.4% and the lowest error percentage at 0.02%. For instance, when the mass flow rate was 0.01 kg/s and the solar radiation was estimated at 1000 W/m², we obtained a thermal efficiency of DPSAH at 88.2%. Additionally, the outside air temperature was estimated at approximately 105.768 °C.

The digital model was used to evaluate the influence of factors on the efficiency of DPSAH such as incident solar radiation, height, ambient temperature as well as various fluid flow rates.
Where the lower the mass flow rate, the higher the output temperature, and the greater the length of the Collector, solar radiation, and the incident ambient temperature, the higher the output temperature

The results of this study represent a significant contribution to enriching knowledge and research on forced convection within channels, especially in the context of solar air collectors and the study also provides new insights to improve the design and operation of these collectors to increase their efficiency and reduce their costs.

Abstract

This thesis presents a numerical study on the efficiency of a DPSAH. The research aims to enhance the collector's performance by studying factors influencing its efficiency. Numerical studies were conducted to measure the outlet air temperature of the collector, as well as the temperatures of the glass cover, absorber, and insulation in the DPSAC system. A model for energy balance equations was used and solved using matrix inversion method via Matlab software. The model's accuracy was verified by comparing numerical results with experimental data from previous research, showing consistency.

The collector length was tested at three different lengths (0.5 m, 1 m, 2 m), with results indicating that a length of 2 m was most effective. Similarly, mass flow rates were tested at different rates, with results showing increased collector efficiency at lower flow rates. A comparison was made between single-pass and DPSAH at the same heat transfer length, indicating that single-pass was superior. Comparisons were also made at the same collector length, confirming that double-pass was the better choice.

The study also provides valuable guidance for selecting the most efficient design standards for DPSAH.

Keywords: solar air heater, single pass, double pass - thermal efficiency, numerical modeling, outlet temperature.

Resumé

Cette thèse présente une étude numérique sur l'efficacité d'un DPSAH. La recherche vise à améliorer la performance du collecteur en étudiant les facteurs influençant son efficacité. Des études numériques ont été menées pour mesurer la température de l'air de sortie du collecteur, ainsi que les températures du couvercle en verre, de l'absorbeur et de l'isolant dans le système DPSAH. Un modèle d'équations de bilan énergétique a été utilisé et résolu à l'aide de la méthode d'inversion de matrice via le logiciel Matlab. L'exactitude du modèle a été vérifiée en comparant les résultats numériques avec des données expérimentales provenant de recherches précédentes, montrant une cohérence.

La longueur du collecteur a été testée à trois différentes longueurs (0,5 m, 1 m, 2 m), les résultats indiquant qu'une longueur de 2 mètres était la plus efficace. De même, les débits massiques ont été testés à différentes vitesses, les résultats montrant une augmentation de l'efficacité du collecteur à des débits plus faibles. Une comparaison a été faite entre le dispositif à simple passage et le DPSAH à la même longueur de transfert de chaleur, indiquant que le dispositif à simple passage était supérieur. Des comparaisons ont également été réalisées à la même longueur de collecteur, confirmant que le DPSAH à double passage était le meilleur choix.

L'étude fournit également des orientations précieuses pour sélectionner les normes de conception les plus efficaces pour les DPSAH.
Mots clés : aérotherme solaire, simple passage, double passage, efficacité thermique, modélisation numérique, température de sortie

الملخص

تقدم هذه الأطروحة دراسة عددية لكفاءة مجمع الهواء الشمسي المزدوج المسار. يهدف البحث إلى تعزيز أداء المجمع من خلال دراسة العوامل المؤثرة على كفاءته. أجريت دراسات عددية لقياس درجة حرارة الهواء المخرج من المجمع وكذلك درجات حرارة الزجاج والممتص الحراري والعازل في نظام DPSAC. تم استخدام نموذج لمعادلات توازن الطاقة وحلها باستخدام طريقة قلب المصفوفة عبر برنامج Matlab. وتم التحقق من صدق النموذج من خلال مقارنة النتائج العددية مع النتائج التجريبية للأبحاث السابقة، مما يدل على تطابقها. تم اختبار طول المجمع على ثلاثة أطوال مختلفة (0.5 م، 1 م، 2 م)، وأظهرت النتائج أن طول 2 متر كان الأكثر فعالية. وبالمثل، تم اختبار معدل التدفق الكتلي بمعدلات مختلفة، وكانت النتائج تشير إلى زيادة في كفاءة المجمع مع انخفاض في معدل التدفق. وتم مقارنة بين مجمع الهواء الشمسي احادي المسار ومزدوج المسار في نفس طول انتقال الحرارة وتبين ان احادي مسار هو أفضل وقارنا بينهما في نفس طول المجمع وتبين ان ثنائي المسار هو الافضل.

تشير الدراسة أيضًا إلى أن النتائج توفر إرشادات قيمة لاختيار معايير التصميم الأكثر كفاءة لمجمعات الهواء الشمسية ذات المسار المزدوج.

الكلمات المفتاحية: سخان هواء شمسي، مسار احادي ،مسار مزدوج- الكفاءة الحرارية، النمذجة العددية، درجة الحرارة المخرج

References

1. Choudhury, P.K. and D.C. Baruah, *Solar air heater for residential space heating.* Energy, Ecology and Environment, 2017. **2**: p. 387-403.
2. Fudholi, A., et al., *Review of solar dryers for agricultural and marine products.* Renewable and sustainable energy reviews, 2010. **14**(1): p. 1-30.
3. Machi, M.H., I. Farkas, and J. Buzas, *Enhancing solar air collector performance through optimized entrance flue design: A comparative study.* International Journal of Thermofluids, 2024. **21**: p. 100561.
4. Benabdelkarim, B. and A. Benatillah, *Etude et simulation de l'effet des paramètres climatiques (température, poussière…) sur les modules solaires en couches minces en région saharien.* Uraer. Cder. Dz, 2016: p. 1-5.
5. Kabir, E., et al., *Solar energy: Potential and future prospects.* Renewable and Sustainable Energy Reviews, 2018. **82**: p. 894-900.
6. BENATIALLAH, D. and A. BENATIALLAH, *Détermination du gisement solaire par imagerie satellitaire avec intégration dans un système d'information géographique pour le sud d'Algérie*, 2019, Université Ahmed Draïa-Adrar.
7. AISSAOUI, F., *Contribution à l'étude de transfert de chaleur d'un capteur solaire placé dans un climat aride: cas de la région de Biskra*, 2017, Université Mohamed Khider-Biskra.
8. El Mghouchi, Y., et al., *Estimate of the direct, diffuse and global solar radiations.* Int J Sci Res, 2014. **3**: p. 1449-1457.
9. Razak, A., et al., *A performance and technoeconomic study of different geometrical designs of compact single-pass cross-matrix solar air collector with square-tube absorbers.* Solar Energy, 2019. **178**: p. 314-330.
10. Ndiaye, M.M.D., *Optimisation d'un capteur solaire double passe à air et estimation des échanges de chaleur paroi-fluide*, 2018, Université Bourgogne Franche-Comté; Université Cheikh Anta Diop (Dakar).
11. Chabane, F., et al., *Collector efficiency by single pass of solar air heaters with and without using fins.* Engineering journal, 2013. **17**(3): p. 43-55.
12. Singh, V.P., et al., *Double Pass Solar Air Heater: A Review.* Int. J. Energy Resour. Appl., 2022. **1**(2): p. 22-43.
13. LABED, A., *Contribution à l'étude des échanges convectifs en régime transitoire dans les Capteurs Solaires Plans à air; Application au Séchage des produits agro-alimentaires*, 2012, UNIVERSITE MOHAMED KHIDER BISKRA.
14. Krarti, M., *Energy efficient systems and strategies for heating, ventilating, and air conditioning (HVAC) of buildings.* Journal of Green Building, 2008. **3**(1): p. 44-55.
15. Karim, M. and M. Hawlader, *Development of solar air collectors for drying applications.* Energy conversion and management, 2004. **45**(3): p. 329-344.

16. VijayaVenkataRaman, S., S. Iniyan, and R. Goic, *A review of solar drying technologies.* Renewable and Sustainable Energy Reviews, 2012. **16**(5): p. 2652-2670.
17. Tchinda, R., *A review of the mathematical models for predicting solar air heaters systems.* Renewable and Sustainable Energy Reviews, 2009. **13**(8): p. 1734-1759.
18. Kabeel, A.E., et al., *Solar air heaters: Design configurations, improvement methods and applications – A detailed review.* Renewable and Sustainable Energy Reviews, 2017. **70**: p. 1189-1206.
19. Alam, T. and M.-H. Kim, *Performance improvement of double-pass solar air heater – A state of art of review.* Renewable and Sustainable Energy Reviews, 2017. **79**: p. 779-793.
20. Assadeg, J., et al., *Energetic and exergetic analysis of a new double pass solar air collector with fins and phase change material.* Solar Energy, 2021. **226**: p. 260-271.
21. Belloufi, Y., et al., *Thermal Performance of Double Pass Solar Air Collector: Numerical and Experimental Investigation.* Annals of West University of Timisoara-Physics, 2023.
22. Pramanik, R.N., et al., *Performance analysis of double pass solar air heater with bottom extended surface.* Energy procedia, 2017. **109**: p. 331-337.
23. Ho, C.-D., et al., *Device performance improvement of recycling double-pass cross-corrugated solar air collectors.* Energies, 2018. **11**(2): p. 338.
24. Condori, M. and G. Duran, *Thermal Efficiency Characterization of a Double-Pass Parallel Flow Solar Air Heater Using a Quasi-Steady Model Under Real Operating Conditions.* Available at SSRN 4634970.
25. Kareem, M., et al., *Performance analysis of a multi-pass solar thermal collector system under transient state assisted by porous media.* Solar Energy, 2017. **158**: p. 782-791.
26. Machi, M.H., et al., *Energy-based performance analysis of a double pass solar air collector integrated to triangular shaped fins.* International Journal of Energy and Environmental Engineering, 2022. **13**(1): p. 219-229.
27. Salih, M.M.M., et al., *An experimental investigation of a double pass solar air heater performance: A comparison between natural and forced air circulation processes.* Solar Energy, 2019. **193**: p. 184-194.
28. Singh, S., *Experimental and numerical investigations of a single and double pass porous serpentine wavy wiremesh packed bed solar air heater.* Renewable Energy, 2020. **145**: p. 1361-1387.
29. Sajawal, M., et al., *Experimental thermal performance analysis of finned tube-phase change material based double pass solar air heater.* Case Studies in Thermal Engineering, 2019. **15**: p. 100543.
30. El Khadraoui, A., et al., *Thermal behavior of indirect solar dryer: Nocturnal usage of solar air collector with PCM.* Journal of cleaner production, 2017. **148**: p. 37-48.
31. Wang, D., et al., *Evaluation of the performance of an improved solar air heater with "S" shaped ribs with gap.* Solar Energy, 2020. **195**: p. 89-101.

32. Fudholi, A., et al., *Performance and cost benefits analysis of double-pass solar collector with and without fins.* Energy conversion and management, 2013. **76**: p. 8-19.